Ampacity Estimation of Medium Voltage Cables for Changing Load Profiles and Uncertain Site Conditions

Master Thesis

Delft University of Technology

AMPACITY ESTIMATION OF MEDIUM VOLTAGE CABLES FOR CHANGING LOAD PROFILES AND UNCERTAIN SITE CONDITIONS

Master Thesis

to obtain the degree of Master of Science
in Electrical Engineering
at the Delft University of Technology,
to be defended on 13-12-2022 at 09:00.

by

B.J.M. CROOIJMANS

Master Student Electrical Power Engineering,
Technische Universiteit, Delft, the Netherlands.

Thesis Commitee & External members:

Dr. Ir. José L. Rueda Torres	TU Delft, Supervisor, Chair
Dr. Ir. Pedro P. Vergara	TU Delft, Daily Supervisor
Dr. Ir. Mohamad Ghaffarian Niasar	TU Delft, Committee
Dr. Ir. Edward J. Coster	Stedin, Daily Supervisor
Ing. Hugo Vergnes	Stedin, Daily Supervisor

Front: A picture that captures the placement of three single-core XLPE medium voltage cables in trefoil formation in the ground.

An electronic version is available at:
http://repository.tudelft.nl/.

SUMMARY

Climate agreement goals set by the Dutch government increase the urge to reduce our greenhouse gases. To fulfil these goals on a residential level a reduction of the emission of carbon which is produced during household demand and transportation (commute) is required. On a residential level, the amount of photovoltaic systems (PV) and electric vehicles (EV) is increasing rapidly to meet these requirements. All these individual changes in the low voltage (LV) grid will have an impact on the aggregated load profile in the medium voltage (MV) network.

The MV network consists of underground cable connections, which play a vital role in the transmission and distribution of electrical power. Currently, the distribution network operator (DNO) uses a fixed ampacity which is based on fixed site conditions to rate their MV cables. The current methodology only considers the current peak of the load profile, but the ampacity of a cable connection is governed by its temperature.

Ampacity ratings for MV cables are specified for a continuous load applied on the specific underground MV cable in certain ambient conditions. When a cyclic load profile is applied the temperature of the cable will not remain constant over a 24 hour load cycle. Since this introduces moments of lesser loading the underground cable has moments during its load cycle to be able to cool down. If this method is applied the whole load profile which is applied on the MV cable could be raised by a factor so that the peak of the profile safely exceeds the nominal ampacity, but stay within the specified thermal limits.

The area in which the DNO operates is quite expansive, the material surrounding the underground MV cable connection will differ for each area. There is a big uncertainty in terms of ground conditions for the majority of the MV cables. The effect that this has on the ampacity of the cable connection will be examined. By running multiple simulations with different ambient conditions, the impact that this uncertainty has on the ampacity can be concluded.

The simulations will be done with an analytical- and a finite element model (FEM). With these models, the effects of uncertain ground conditions and the possibility to use an cyclic rating factor for specific load profiles can be calculated. This will be used to study the impact of the changing cyclic load profile due to the increase of PV and EV in the network. The interplay between these factors is interesting since the uncertain ground conditions have a negative impact on the overall ampacity while the cyclic rating factor can (partly) compensate for this loss.

SAMENVATTING

De door de Nederlandse overheid gestelde doelen in het klimaatakkoord versterken de drang om onze broeikasgassen te verminderen. Om deze doelen op residentieel niveau te bereiken, is een vermindering nodig van de broeikasgassen die worden geproduceerd tijdens het verbruik van energie voor huishoudens en transport (woon-werkverkeer). Om aan deze eisen te voldoen, neemt het aantal fotovoltaïsche (PV) systemen en elektrische voertuigen (EV) toe. Al deze individuele veranderingen in het laagspanningsnet zullen een impact hebben op het geaggregeerde belastingsprofiel in het middenspanningsnet.

Het middenspanningsnet bestaat uit ondergrondse kabelverbindingen, die een cruciale rol spelen bij de transmissie en distributie van elektriciteit. Momenteel gebruikt de netbeheerder een vaste toelaatbare stroom voor de middenspanningskabel verbindingen die gebaseerd is op vaste grondeigenschappen. De huidige methodologie houdt alleen rekening met de piek van een belastingsprofiel, maar de daadwerkelijke belastbaarheid van een kabelverbinding wordt bepaald door de temperatuur.

De belastbaarheid van ondergrondse middenspanningskabels is gespecificeerd voor een continue toelaatbare stroom in bepaalde vastgestelde grondeigenschappen. Wanneer een cyclisch belastingsprofiel wordt toegepast, zal de temperatuur van de kabel niet constant blijven gedurende de dagbelastingscurve van 24 uur. Dit creëert momenten van mindere belasting, hierdoor heeft de ondergrondse kabel tijdens zijn belastingspatroon momenten om af te koelen. Als deze methode wordt toegepast, kan het volledige cyclische belastingspatroon op de middenspanningskabel met een factor worden verhoogd, zodat de piek van het profiel veilig de nominale toelaatbare stroom overschrijdt, maar de kabelverbinding binnen de gespecificeerde thermische limieten blijft.

Het gebied waarin de netbeheerder opereert is vrij uitgestrekt, de grondeigenschappen rondom de ondergrondse kabelverbinding zullen per gebied verschillen. Er is een grote onzekerheid in termen van grondeigenschappen voor de meeste middenspanningskabels. Onderzocht wordt welk effect deze onzekerheid heeft op de belastbaarheid van de kabelverbinding. Door meerdere simulaties uit te voeren met verschillende omgevingscondities, kan de impact die deze onzekerheid heeft op de toelaatbare stroom worden bepaald.

De simulaties zullen uitgevoerd worden met een analytisch model en een eindige-elementenmethode. Met deze modellen kunnen de effecten van de onzekerheid van de bodemeigenschappen en de mogelijkheid van een cyclische belastbaarheid voor een specifiek belastingspatroon worden berekend. Dit zal worden gebruikt om de impact te bestuderen van het veranderende cyclische belastingsprofiel als gevolg van de toename van PV en EV in het netwerk. Het samenspel tussen deze factoren is interessant aangezien de onzekere bodemeigenschappen een negatieve invloed hebben op de toelaatbare stroom, terwijl de cyclische belastbaarheidfactor dit verlies deels kan compenseren.

Contents

List of Symbols

The symbols used and the quantities which they represent are given in the following list:

c_p	Specific volumetric heat capacity of the material	J/m^3K
C	Electrical capacitance per cable core	F/m
d_c	Diameter over conductor	m
D_a	Diameter over armour	m
D_i	Diameter over insulation	m
D_s	Diameter over screen, inner diameter of the covering	m
D_e	Diameter over cable, outer diameter of the covering	m
E	Energy	J
Ei	Exponential integral function	
f	System frequency	Hz
I	Permissible current for given (standard) condition	A
I_R	Resistive element of the current	A
I_C	Capacitive element of the current	A
L	Axial depth of burial of a cable	m
m	Mass	kg
M	Cyclic rating factor	
n	Number of conductors in a cable	
M_o, N_o	Coefficients used for calculating cable partial transient temperature rise	s, s^2
Q_a	Thermal capacitance of armour	J/mK
Q_c	Thermal capacitance of conductor	J/mK
Q_i	Thermal capacitance of insulation	J/mK
Q_j	Thermal capacitance of jacket	J/mK
Q_s	Thermal capacitance of sheath	J/mK
Q_A, Q_B	Elements of equivalent thermal circuit	J/mK
r_1	Internal radii of a cylindrical layer	m
r_2	External radii of a cylindrical layer	m
R_{ac}	A.C. resistance of conductor at maximum operating temperature and 50 Hz	Ω/m
R_s	A.C. resistance of sheath at maximum operating temperature and 50 Hz	Ω/m
S	Cross-sectional area of the conductor	m^2
T	Thermal resistance of material	$K \cdot m/W$
T_1	Thermal resistance per core between conductor and sheath	$K \cdot m/W$
T_2	Thermal resistance between sheath and armour	$K \cdot m/W$
T_3	Thermal resistance of external serving	$K \cdot m/W$
T_4	Thermal resistance of surrounding medium	$K \cdot m/W$

T_A, T_B	Elements of equivalent thermal circuit	$K \cdot m/W$
T_a, T_b	Apparent thermal resistances used to calculate cable partial transient temperature rise	$K \cdot m/W$
t_1	Thickness of insulation between conductor and sheath	m
t_2	Thickness of the bedding	m
t_3	Thickness of the serving	m
U_0	Voltage between conductor and screen or sheath	V
W	Amount of heat generated within a body	W/m
W_c	Losses in conductor per unit length	W/m
W_d	Losses in dielectric per unit length	W/m
W_l	Total loss per unit length	W/m
W_s	Losses dissipated in sheath per unit length	W/m
W_{in}	Energy rate entering the cable	W
W_{loss}	Energy rate internally generated in cable	W
W_{out}	Energy rate dissipated by the cable to its surrounding	W
W_{store}	Energy rate stored inside the cable	W
X	Reactance of sheath	Ω/m
ρ	Thermal resistivity of material	$K \cdot m/W$
ρ_T	Soil thermal resistivity	$K \cdot m/W$
ρ_d, ρ_w	Thermal resistivity of dry and moist soil respectively	$K \cdot m/W$
θ	(Maximum) operating temperature of the conductor	$°C$
$\Delta\theta$	Temperature rise of the conductor above ambient temperature	$°C$
θ_a	Initial ambient temperature of the medium surrounding the cable	$°C$
θ_c	Conductor temperature rise above the outer surface of the cable	$°C$
θ_e	Cable outer surface temperature rise above ambient temperature	$°C$
θ_x	Temperature	$°C$
$\Delta\theta_x$	Temperature rise	$°C$
θ_R	Temperature of the conductor, when a continuous load (100% load factor) is applied	$°C$
δ	Thermal diffusivity	m^2/s
$\tan\delta$	Loss factor of insulation	
τ	Time constant (tau)	s
μ	loss-load factor of a load profile	
a, b	Coefficients used for calculating cable transient temperature rise	$1/s$
p	Factor to divide the thermal capacitance of the dielectric	
v	Ratio of the thermal resistivity of dry and moist soil	
Y_i	Ordinate of an hourly load pulse squared of a 24 hour load profile	
λ_1, λ_2	ratio of respectively sheath and armour to the total conductor loss	
α	Attainment factor for the conductor to cable surface temperature rise	
t	time from start of application of heat in seconds	s
i	time from start of application of heat in hours (i=3600t)	h
k	Ratio of the cable outside surface temperature rise above ambient to conductor temperature rise above ambient under steady conditions	

1

INTRODUCTION

The Netherlands set a goal in its national Climate Agreement [1], to reduce the emission of CO_2 in 2030 by 49% compared to 1990. To realise this change a lot of processes which now heavily rely on gas and fossil fuels will be transformed to work on electricity. This change is not only happening in the industry, electrification is taking place in all places. With the rising gas prices and people's mindset to be more sustainable, electrification is also taking place at a large pace in residential areas. The number of electric vehicles (EV) and solar systems (PV) in residential areas is rising very rapidly. A prognosis done by ElaadNL [2] shows the expected rapid growth of EVs in the Netherlands. The prediction is that the share of EVs in the total population of passenger cars will rise from the current 3.4% to 98.6% by 2050.

Facilitating electrification requires grid capacity, distribution network operators (DNO) are having a hard time keeping up with the pace of this increased energy demand and generation. Currently, extra or reserve grid capacity in some areas of the Netherlands is approaching a minimum. Research conducted by PWC [3] commissioned by Netbeheer Nederland shows an increase in consumption of electricity by 2050 in the sectors of industry, residential and e-mobility of 25-40% compared to 2019. To facilitate this increase in the transportation of power, the calculated annual investment in the grid should be more than doubled by 2050.

In the past, energy got transported from the power stations by the high voltage (HV) grid to all the regions in the Netherlands. Within these regions, the energy gets distributed by the medium voltage network. The final step of transformation is done by a distribution transformer, which creates a low-voltage network within a neighbourhood. More and more distributed energy resources (DER), for instance PV, are present in the low voltage network and the conventional top-down power flow is changing. When there is more generation than consumption in a neighbourhood the net power flow changes direction. This change also has an effect on the MV load profile since all the LV connections are connected through the distribution transformer to the MV network.

This study focuses on the impact that the changing MV load profile has on MV cable ampacity calculations. Ampacity, or current-carrying capacity, is an important parameter in all components used in the electricity grid. The ampacity defines the current which can flow through a component continuously, without violating the maximum temperature of the individual elements inside the component.

Ampacity is influenced by material properties of the surrounding material, grounding technique, placement depth, etc. Some of these factors have a greater effect than others. The focus will be on the ampacity of Medium Voltage (MV) cables. The biggest challenge in defining the ampacity of a cable is the heat build-up due to the current passing through the conductor which has a certain resistivity, this results in losses which produce heat (I^2R), the other losses (e.g. dielectric and sheath) will further increase this effect.

Cable ampacity is a subject that has been studied for quite some time. The studies date back almost one hundred years, for example with the work of D.M. Simmons (1932) [4] which has been extended 25 years later by J.H. Neher & M.H. McGrath (1957) [5]. These papers and the ones that followed formed the basis on which the standards which are used today are based, e.g. the IEC60287 and the IEC60853.

In [6] the relationship between current and thermal response is examined. The conclusion states that to precisely predict the temperature rise at certain loads many variables have to be considered. The computational power of computers is increasing over the last few years, this gives the ability to do more precise studies. When correction factors and assumptions are used to calculate the temperature a certain error is introduced. In this research, the impact that a changing load profile and certain assumptions have on the ampacity will be studied.

1.1. BACKGROUND

In the past and up to a certain extent today, the daily load profile was predictable. Due to the rapid penetration of DER, EV, PV, etc. in the electricity network the aggregated load profile in the MV grid is changing at a fast pace and is becoming less predictable. The total energy demand of the Netherlands is rising, but the grid is not growing at an equal pace.

The current load profile has some moments of lesser loading in which the components in the grid have the ability to cool down. The load profile in the MV grids changes due to the technologies mentioned above and load shifting. Load shifting can reduce demand peaks by shifting demand to another moment in time when congestion happens. The same amount of energy is still being transported but at a later or earlier time instant. When this is further optimized the possibility may arise that cables are continuously loaded at a certain load factor.

On the other side, DNOs are becoming more aware that knowing the real-time ampacity of components is becoming more important. The assets inside the network in the not so far future will be operated on the edge of their limits due to congestion events.

In order to know up to which point components can be stressed, models need to be used to estimate the ampacity of components under certain conditions, like operational, weather and ambient factors. Just relying on plain estimations may render a decision that can lead to excessive fatigue (reduced lifetime), outage or not optimal use.

In the past, cable connections were oversized for the power demand that was present that day. A significant amount of the cable network from the DNOs is over 30 years old. These connections are still operational and also need to cope with the increasing demand and changing load profiles. Since the ampacity limit of the MV cables is being approached or is unknown, it is becoming more and more important to accurately know these limits. To calculate these limits extra models and measurements are needed.

Article [7] neatly describes the urgent need for dynamic models for utility companies since they have to manage many cables inside their grids that last for decades. The ampacity which stands for the current carrying capacity of a cable is mostly only determined at the installation of a cable. In some scenarios, this includes the models and assumptions from decades ago that are still being used. Stationary ampacity calculations and assumed soil conditions could differ from the insight we have nowadays. The computational power of machines has vastly improved and there are more accurate methods to determine the ground conditions, together with dynamic models a more accurate ampacity can be determined. Dynamic rating techniques allow cables to be loaded above their stationary ampacity for a certain period of time, article [7] describes the following benefits that can be obtained by dynamic modelling, which are beneficial for the DNOs:

- Just-in-time investment
- Increasing network flexibility
- Better knowledge
- More possibilities to solve network contingencies
- A more intelligent way of network operation

The major factors affecting cable ampacity are different for different installation types; underground, air and riser poles [8]. Since the entire MV cable network of DNOs in the Netherlands is buried the focus will be on this installation type. The main factors in this type of installation that affect the ampacity are cable calibre, soil thermal resistivity and bonding method [8]. These factors have an influence on the dynamic thermal rating which in turn has an effect on the ampacity of the component, the ampacity of a cable connection is mainly governed by the thermal limits of the materials used.

1.2. PROBLEM STATEMENT

Traditionally, the DNO had to deal with predictable daily and annual load profiles and predictable annual growth rates for power demand. MV cable connections were operated well within their limits and due to this, it was not needed to model the cable connections to their full extent. It was common practice to use standardized ampacity tables from the standards or the brochure of the manufacturer. The DNO looks at the maximum peak inside a load profile, this peak demand must not exceed the ampacity value which is specified by the manufacturer. This method to determine the ampacity of an underground MV cable is not dependent on dynamic models, ground parameters or the shape of the load profile. This methodology is not feasible anymore because the DNO are looking into the possibilities to maximize the usage of their assets to make the energy transition possible.

Currently, the load profiles in MV cable connections are subject to significant change and it is anticipated that this change will continue in the future. Due to these changes and the fact that grid redundancy cannot be abandoned, components are being utilised close to their expected maximum ampacity. Since the MV cable network is operated closer to its technical limit it is becoming more important to know these limits accurately for different circumstances. Due to these changes it no longer suffices to use a standard ampacity table during grid planning. For the MV cable network to stay within the limits, a more realistic ampacity for different conditions is significantly becoming more important. Due to the fixed value used for the ampacity, there is uncertainty if the conditions belonging to these fixed values are met in reality. Therefore there is a possibility that the ampacity of a cable connection is under or overestimated. The newly obtained ampacity might differ slightly or in some cases heavily from the current ampacity used by the DNO. If these changes are neglected this may have a drastic impact on the lifetime and reliability of the MV cable system.

Moreover, it is also important to know the computational error that is present due to simplifications and assumptions during analytical modelling. When these factors are taken into account a more realistic ampacity for underground MV cable connections could be determined.

1.3. Objective & Research Questions

The goal of this research is to gain additional insight into the ampacity of the MV network and identify the impact that a changing load profile and uncertain site conditions have. A sensitivity analysis of the used parameters will give insight into the computational error, this will create awareness for future projects. Furthermore, this gives a view of where to lay the emphasis on future measurements in the field.

How the aggregated future load profile will be shaped is a big uncertainty, but by running different scenarios this uncertainty could be partly mitigated. The goal is not to create a load profile which will showcase the future but see what the impact is going to be on the ampacity of MV-cable connections from the rapid growth of PV systems and EVs. How does the thermal response of a cable system alter when the shape of the load profile changes? Aggregated load profiles of households, PV systems and EVs are used to create case studies with differently shaped 24-hour load profiles.

When the shape of the load profile and more accurate ground conditions are incorporated into the model, a closer to reality cable ampacity can be determined. By knowing the limits of the ampacity, cable systems can be utilized to their full potential without reducing their lifetime. The main factor that determines the ampacity of a cable is the temperature constraint of the conductor or the sheath. Since most thermal processes have a high time constant, the thermal responses are quite slow. When a cable connection is loaded with a load profile there are moments of high loading where the cable will tend to warm up and moments of less loading that give the cable the ability to cool down. When this process is incorporated in the determination of the maximum cable ampacity the peak of the load profile might exceed the nominal loading of the cable for a short period of time. This can happen due to the high time constant (slow reaction time) and if there are moments in the load profile of less loading when the cable has the ability to lose some of its extra generated heat. The thermal limits still hold and will be the limiting factor.

A cable connection crosses a lot of different soil compositions and every now and then has to cross an obstacle. Those obstacles could be intersections in which the cable will be placed in a duct. For cable connections, the worst case or hot spot of the whole connection is considered, since this will be the limiting factor for the ampacity of the whole connection.

The objective of this research is to gain deeper insight into the ampacity of MV cable connections when the load profile changes and the site conditions are unknown. This will be done using an analytical model which will be validated using a finite element model. The input of the model will change and the impact that these changes have on the output will be examined. The research will try to answer the following questions:

- What is the impact of different load profiles (case studies) due to changing loads and distributed generation (e.g. PV) on the ampacity of MV cables?
- Which variables of the model have the most impact on the ampacity and overloading capabilities of MV cables?
- Which assumptions can be taken to simplify the method and still have a representative outcome?
- Which field measurements need to be taken to increase accuracy and aid with validation of modelling the ampacity of MV cable connections?

1

1.4. OUTLINE

A brief description of the information found in each chapter.

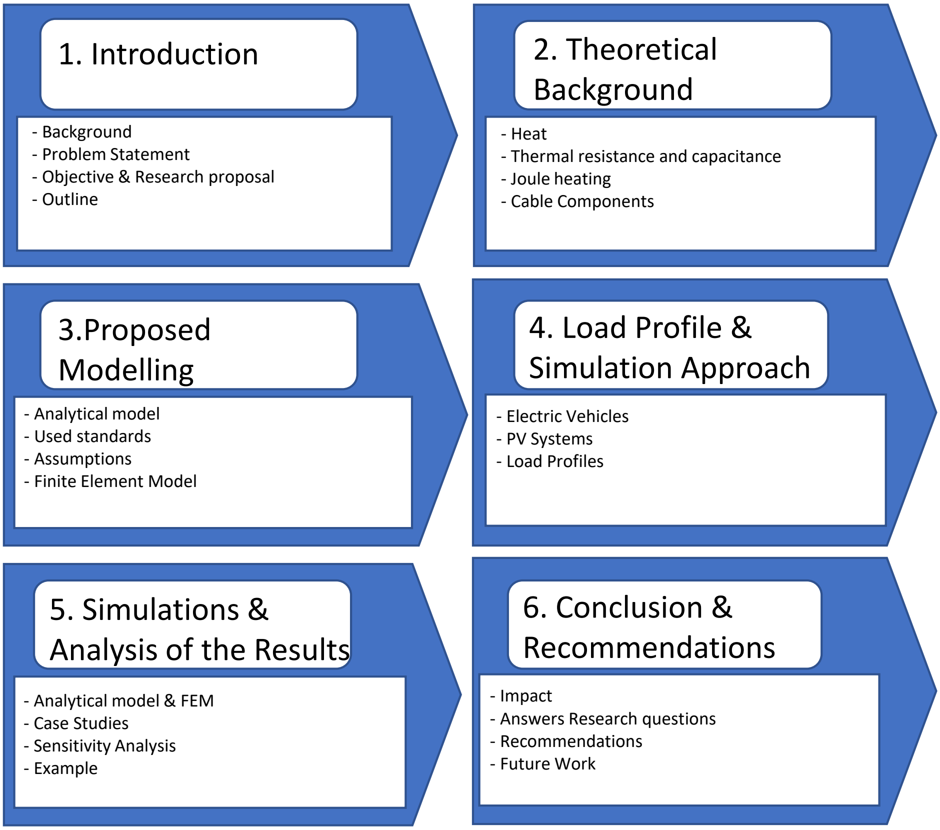

Chapter 1: **Introduction**
The problem will be stated with a background of why this problem is relevant at this moment. The currently used method used by the DNO to tackle this problem and the research proposal to have new insights into the way ampacity could be determined in the future.

Chapter 2: **Basics of Cable Thermal Behaviour**
The chapter begins with basics on thermal resistance and how Joule heating takes place. It continues with the structure of the different cable components and the ambient conditions, and their contribution to the total heat transfer.

Chapter 3: **Proposed Modelling of Cable Thermal Behaviour**
This chapter describes how all the different cable components come together to form an

analytical thermal model of a cable in the ground. How the IEC60287 and the IEC60853 could be used together to make a proper ampacity calculation for a repetitive load profile. A FEM model is constructed of the same cable structure. The assumptions that are made due to the missing measurement data and the simulation software used.

Chapter 4: **Load Profile & Simulation Approach**
The growth prediction and problem statement will be evaluated for the penetration of PV and EV in the network. Load profiles are created to simulate the effect that growth predictions of PV and EV have on the ampacity of a MV cable. The effect that congestion management has on the overloading capabilities in the MV grid is examined using an arbitrary load profile which tries to maximize grid utilization. Using this technique the impact that the changing shape of the load profile has on the ampacity of a MV cable can be studied.

Chapter 5: **Simulations & Analysis of the Results**
Steady-state and transient simulations are computed to study the ampacity and temperature response, with a certain set of input parameters. A comparison is made between the analytical and the finite element model. The results of the different case studies are being studied and a theoretical example of MV cable loading is simulated. Due to missing measurements and data, sensitivity analyses are done to see the impact of each parameter and the potential gain of field measurements.

Chapter 6: **Conclusion & Recommendations**
Answers to the research questions and conclusions are given in this chapter. Recommendations are made in which field the DNO has to improve its measurements to fully utilize its grid capacity and increase modelling accuracy. Recommendations are formulated for future work to gain even more insight into this topic.

2

Theoretical background of the study of Cable Thermal Behaviour

A MV cable is made up of different layers and materials, these layers and materials all have their own purpose and property. To analyse the thermal behaviour of an underground cable it needs to be modelled to such an extent that the effect that each layer has on the total thermal response is taken into account. This chapter describes the construction of the cable and will discuss the need for all different layers in the cable and how to model them for a stationary and transient thermal response. To calculate the ampacity of a cable the heat transfer equations needs to be solved, this defines the relationship between the current passing through the conductor and the temperature in the cable and its surrounding. The focus will be on single-core XLPE cables without armouring, which are common for grid operators in the Netherlands. Some analyses are also done for a PILC cable to make a comparison between the different cable types. PILC cables were used in the past but are still operational today. The XLPE cable used in this research is the TKF single-core AL 240mm^2 12/20kV placed in trefoil and the PILC cable is the NKF three-core CU 120mm^2 10kV. Since the PILC cables are not being used in new projects and are being phased out, the emphasis of this research is on the XLPE cable.

All the different layers are described in Section 2.2, as described above all layers serve a purpose to make energy transport possible. When looking at the thermal behaviour of a cable, some layers have a very minimal effect on the overall result and can be removed from the model to simplify the computation. In section 2.1 the basics of thermal dynamics which are needed to simulate the thermal response of a cable in the ground are represented. Each individual layer has its influence on heat production or transfer. The figure also pinpoints the heat sources W, thermal resistances T and thermal capacitances Q.

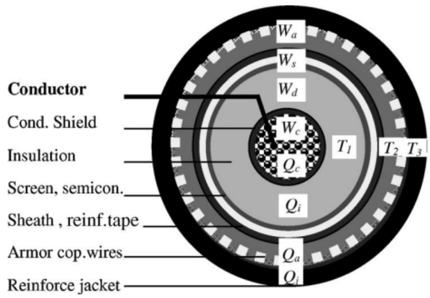

Figure 2.1: Cross section of a single core cable [9]

2.1. FUNDAMENTALS OF THE ANALYTICAL STUDY APPROACH

Heat transfer occurs when there is movement of atoms and molecules, when the movement of these atoms and molecules increases so does the heat energy inside the material. The average energy of the molecules and atoms in a given material or system determines the temperature. The progression of heat in an object or system can take place in three different ways, namely radiation, conduction and convection.

- **Radiation**, if no physical contact is present between two objects but there is transfer or exchange of heat between the two objects. The heat travels in the form of electromagnetic waves in the infrared spectrum.
- **Conduction**, takes place by direct contact of two objects. The temperature difference will cause the energy to transfer.
- **Convection**, takes place in fluids. The cause of the heat transfer is the difference in density.

In a XLPE cable, the heat progresses by conduction, since the different layers inside the cable are touching and it is not surrounded by fluids, except when the cable is placed in groundwater.

If there is a temperature difference (gradient) within a certain body or volume, the temperature will tend to level out. The heat of the hotter parts will flow to the colder parts until an equilibrium is reached. This is process is described by partial differential equations. For instance, in the modelling of the temperature within a very thin metal bar as a function of position and time, the time-dependent one-dimensional equation will be Equation 2.1. Since it is a very thin metal bar the heat will only propagate in the x direction.

$$\frac{\partial \theta_x}{\partial t} = \delta \frac{\partial^2 \theta_x}{\partial x^2} \tag{2.1}$$

Where x is the position, t is the time, θ_x is the temperature and δ is the thermal diffusivity. These heat equations require a lot of computational power and are complex. Analytical solutions to the heat transfer equations are at hand for simple cable constructions and conditions. For a cable connection this is done in a two-loop representation of a cable circuit (Section 3.1), this turned out to be quite accurate for most practical applications [10]. This is also favourable for the DNO since the amount of MV cables in their network is very high, it is beneficial to have a fast and representative outcome.

There is a linear relationship between the current passing through a conductor and the voltage over the conductor. This linear relationship is called electrical resistance, the same principle applies to heat flow. The linear relationship is heat flow through a material which causes a temperature difference in the material, due to the thermal resistance.

Figure 2.2: Analogy electrical and heat conduction

$$U_1 - U_2 = I \cdot R \tag{2.2}$$

$$\ominus_1 - \ominus_2 = W \cdot T \tag{2.3}$$

Conduction of heat can be described similar to electrical conduction. A resistance sits in a flow of current or heat. In the case of electrical conduction, an electrical resistance sits in the electrical current path creating a voltage drop over the resistor, Equation 2.2. The same happens with heat, heat flow (W) passes through a thermal resistance creating a temperature drop, Equation 2.3. This analogy is visualised in Figure 2.2. Using this familiarity with lumped parameters to solve differential equations representing current flow in an object which has a potential difference, the same could apply to simple heat conduction problems. The problem begins by dividing the object into multiple smaller volumes, each of which has a certain thermal resistance (Section 2.1.1) and thermal capacitance (Section 2.1.2).

To let a solid, gas or liquid rise in temperature energy is needed. Every object reacts differently to the energy you put into it, also the amount of energy needed to warm an object differs. The amount of energy needed depends on three factors:

- The mass or volume of the object [m]
- The rise in temperature [$\Delta\theta_x$]
- The specific heat capacity of the material [c_p]

The mass or volume of an object determines the scale of the object on which energy is applied to heat up the object. The temperature rise gives the difference in temperature between the state when the energy is applied to when the energy is switched off and the end temperature is reached or when an equilibrium is reached. The specific heat of material connects these two quantities, the amount of energy (Joule) needed to heat 1 m^3 of material by 1 °C.

$$\Delta E = m \cdot c_p \cdot \Delta\theta_x \tag{2.4}$$

2.1.1. THERMAL RESISTANCE

Thermal resistance reassembles the ability of a surrounding to dissipate its produced heat. This gives a measure of the ability of the material to impede heat flow. The unit for thermal resistance is Kelvin meter per Watt [$\frac{Km}{W}$]. The uniform thermal resistance per unit length for conduction of heat of a cylindrical layer is calculated using Equation 2.5. With this Equation and the generated heat, the temperature difference can be calculated using Equation 2.3.

$$T = \frac{\rho}{2\pi} \ln \frac{r_2}{r_1} \tag{2.5}$$

If the thermal resistance surrounding a heat source is low, it is able to dissipate the produced heat easier than when the thermal resistance is high. The thermal resistance of the different materials in a cable is quite stable and uniform. For the medium surrounding the cable for instance soil, the thermal resistance may differ over the trajectory of the cable. It will also differ over the lifespan of the cable, since the soil thermal resistance is highly dependent on the moisture content inside the soil, see Section 2.3. Since the thermal resistance can differ over the trajectory of the cable it is important to know the bandwidth of the thermal resistance to determine the ampacity of the cable. How the thermal resistivity of the surrounding affects the cable ampacity is further explained in Section 5.1.1.

2.1.2. THERMAL CAPACITANCE

Thermal capacity is the value that represents the amount of heat needed to raise the temperature of the material by one Kelvin. This gives a measure of the material's ability to store heat. The unit for thermal capacitance is Joule per meter Kelvin [$\frac{J}{mK}$].

When the thermal capacitance is combined with the thermal resistance, the heat flow can be modelled as an analogous RC electrical circuit. Heat capacity is needed in the model to simulate the time response of the system, this can not be done using only the thermal resistance of the system. Most cable rating issues are time-dependent, for example, when a cable is constantly loaded, but during a fault or maintenance, the loading is increased to a new level. Meaning that more current will be carried by the circuit which increases loss causing slow changes in the temperature distribution within the MV cable and the material around it.

To obtain the temperature distribution within the cable, the rate of change and the temperature of the surrounding heat transfer equations need to be solved, which contain partial derivatives. In most cases, it can be very difficult and time-consuming to obtain analytical results of these equations. When the temperature gradient within a body is small enough a lumped capacitance method could be applied. This method is very well suited for analytically solving cable ampacity calculations. The only drawback is that larger bodies (e.g. insulation/dielectric) must be subdivided into smaller sections. The newly obtained solid body needs to be small since the assumption is made that the temperature within the body is spatially uniform, so there is no internal temperature gradient at any moment in time. Then the thermal capacitance can be obtained by multiplying the area of the cylindrical shape with the specific volumetric heat capacity of the material (Equation 2.6).

$$Q = \frac{\pi}{4}(D_2^2 - D_1^2)c_p \tag{2.6}$$

2.1.3. JOULE HEATING

When a voltage and a current are applied on a cable, the electric field will build up between the conductor and the sheath and the magnetic field will circulate around the conductor. These two fields are perpendicular to each other at any point in space. The energy passing through the conductor in the direction of the conductor is perpendicular to the plane which is spanned by the electric and magnetic fields. This vector is also known as the Poynting vector, it represents the directional power flow.

Due to the linear relationship described at the beginning of this Chapter, there is also a voltage drop over the conductor, since the conductivity of the conductor is not infinite. This voltage drop creates a small electric field in the direction of the power flow. This electric field is small compared to the electric field which is present between the conductor and the sheath, which is pointing radially outwards. The small electric field which is caused by the voltage drop over the conductor together with the circulating magnetic field also spans a plane. Perpendicular to this plane is a Poynting vector which faces radially inwards inside the conductor. Since the direction of this Poynting vector is not in the direction of the power flow this energy is dissipated in the form of loss (heat). In this case, circuit theory can be applied and it suffices to apply Ohms law to describe the generation of heat with $I^2 \cdot R$ also known as Joule heating.

Joule heating is the effect of electrical energy which is transformed into thermal energy when the energy passes through an object. When considering electrical energy transportation this thermal energy is considered a loss and should be minimized. This minimisation is mainly affected by altering two variables current and resistance, since $P = I^2 \cdot R$. The current can be reduced by for instance choosing a different voltage level and the resistance should be kept as low as possible by picking the right material and conductor cross-section. In MV cable systems two types of materials are used for conducting electricity, namely Copper and Aluminium. The main difference between these two materials is cost and conductivity. Copper is more expensive but has a lower resistance which will produce less heat with the same amount of current passing through it.

2.1.4. Energy Balance

The law of conservation of energy must be taken into account when modelling a thermal process. For a cable, this is described by Equation 2.7, which shows the balance between all energy rates in Joules per second.

$$W_{in} + W_{loss} = \Delta W_{store} + W_{out} \tag{2.7}$$

The left side of the equation shows the amount of energy which will flow into the cable or is dissipated by the cable itself due to losses (Joule and dielectric). This will increase the energy stored within the cable. The outflow of energy will release the stored energy. If the system reached a steady-state condition (equilibrium) the delta stored energy will be zero and the outflow of energy will be equal to the inflow plus the self-generated heat. The rate at which the energy can flow into and out of the cable is proportional to the surface area of the cable.

2.2. Cable Components

A MV cable consists of different layers, a cross-section is given in Figure 2.1. From inside to outside it consists of a conductor, conductor shielding, insulation, sheath, reinforcing tape around the sheath and a jacket. All the layers of a MV cable starting from the centre and moving radially outwards are described in the coming sections. Each layer in a cable has its own purpose and is very important for the functioning of the whole design. The focus will be on how each layer contributes to the stationary and transient thermal behaviour of the cable.

2.2.1. Conductor

The goal of the conductor is to transport the electrical energy from the beginning of the cable to the end. The heat produced in a conductor per unit length is mostly affected by the current passing through the conductor, Equation 2.8. Since the produced heat is dependent on the current squared, the current has a major influence on the thermal behaviour of a cable.

$$W_c = I^2 R_{ac} \tag{2.8}$$

The thermal capacitance of the conductor in the single-core XLPE cable can be calculated by using the volumetric specific heat (c_p) of aluminium times the area of the cross-section of the conductor, see Equation 2.9. The thermal resistance of the conductor is in relationship to the other thermal resistances very small, thus can be neglected.

$$Q_c = S \cdot c_p \tag{2.9}$$

2.2.2. Insulation/Dielectric

Good quality insulation is important for a proper and long lifetime of a cable. In the past multiple forms of insulation are used, for instance oil-impregnated paper, oil pressure and EPR. Nowadays XLPE is the material of choice when designing MV cables. The dielectric layer is the insulation between the conductor and the sheath.

DIELECTRIC LOSS

When a cable is energised dielectric losses are formed in the insulation layer of the cable. An important factor for the magnitude of the loss is the loss angle ($\tan\delta$), Equation 2.10.

$$\tan\delta = \frac{I_R}{I_C} \tag{2.10}$$

The quality and reliability of a cable are determined by the amount of contamination or imperfections in the insulation. Perfect insulation is similar to a parallel plate capacitor where voltage and current are 90 degrees phase-shifted, and the current is only capacitive. Factors like air and moisture pockets or water and electrical trees influence the resistive current (I_R) through the insulation. The aim of a manufacturer is to perfect their cable and manufacturing process to have an almost zero $\tan\delta$. When the amount of contaminations increases so does the resistive current which results in a shift in the $\tan\delta$ in a negative way.

The heat produced by the dielectric loss can be calculated by Equation 2.11.

$$W_d = 2\pi f C U_0^2 \tan(\delta) \tag{2.11}$$

The applied voltage on the conductor influences the total dielectric loss. Since the dielectric loss scales quadratically with the voltage which is present over the dielectric layer, which is the voltage difference between the conductor and the sheath (U_O). In most cases at a lower voltage for instance in distribution, the dielectric loss is neglected. The IEC60287 (Table 3) [11] states that dielectric loss can be neglected when $U_0 < 127kV$. In this research, the contribution of the combined dielectric and sheath loss on the total loss of the analytical model is examined, to estimate what the computational error is.

VAN WORMER COËFFICIENT

In 1951, Buller [12] described a thermal approximation where the dielectric layer is split in half, half of the thermal capacity of the insulation is placed at the conductor with its temperature and half at the sheath at sheath temperature. These two temperatures are different from one other due to the temperature gradient. In 1955, F.C. van Wormer [13] improved this method because in a cable cross-section the thermal capacitance and resistance together with the temperature of the insulation are not linear with the thickness of the insulation in a single core cable. The method developed by van Wormer which is named after its inventor is better suited for this nonlinear behaviour.

The method of Van Wormer is widely used since it gives a good improved approximate solution, compared to a computation which calculated the temperature gradient to its full extent which is complex and time-consuming. An approximate solution combined with the lumped model is sufficient in most cases. The total thermal capacitance of the insulation that needs to be split accordingly is given in Equation 2.12.

$$Q_i = \frac{\pi}{4}(D_i^2 - d_c^2) \cdot c_p \tag{2.12}$$

The Van Wormer coefficient (p) is given for steady state, where D_c and D_i are the outer radii of the conductor and insulation respectively.

$$p = \frac{1}{2ln(\frac{D_i}{D_c})} - \frac{1}{(\frac{D_i^2}{D_c^2}) - 1} \tag{2.13}$$

The van Wormer coefficient p as computed in Equation 2.13 is the factor that determines the portion of the total capacitance which is at the conductor $p \cdot Q_i$ or the sheath $(1-p)Q_i$, taking the non-linearity of the thermal gradient into account.

For transients shorter than one hour a different approach needs to be taken to factor out the total capacitance of the insulation. It is found necessary to divide the insulation into two portions with equivalent thermal resistance. The thermal capacitance is then split using a slightly different equation (2.14).

$$p^* = \frac{1}{ln(\frac{D_i}{d_c})} - \frac{1}{(\frac{D_i}{d_c}) - 1} \tag{2.14}$$

The thermal capacitance of the dielectric is then split into two sections using the van Wormer equations. Since we are interested in longer partial transients of $> \frac{1}{3}T \cdot Q$ and the cyclic rating of MV cables Equation 2.13 is used.

The thermal resistivity of the insulation is calculated using Equation 2.15.

$$T_1 = \frac{\rho}{2\pi} \ln(1 + \frac{2t_1}{d_c}) \tag{2.15}$$

2.2.3. SHEATH

As described in the IEC60287-1-1 [11] the assumed screen losses can be estimated using a portion of the conductor loss. The bonding technique plays an important role in the amount of screen losses inside a cable. The bonding technique of a cable must be known to determine the amount of screen losses. Since the screen losses are induced by the current flowing through the conductor it is logical that the two losses are dependent. The sheath loss can be calculated as a portion of the conductor loss and is calculated using Equation 2.16. This loss factor can be used when three single-core cables are laid in trefoil formation and the sheath is bonded at both ends and no cross-bonding is applied. The sheath loss per single core cable is then obtained using Equation 2.17.

$$\lambda_1 = \frac{R_s}{R_{ac}} \frac{1}{1 + (\frac{R_s}{X})^2} \tag{2.16}$$

$$W_s = \lambda_1 \cdot W_c \tag{2.17}$$

In [14] a comparison of sheath temperature which is measured and calculated is shown. The results look quite promising when comparing the real-time calculated sheath temperature with the measured temperature. The researchers had access to a cable with a glass-fibre temperature monitoring system along the whole trajectory. This greatly helped to validate and see the computational error on the calculated temperature with their developed model. The research does not include the new maximum ampacity of their use case in combination with their stated maximum sheath temperature of 45 [°C] if ground dehydration should be avoided when loading is applied for a longer period of time. It is interesting to see that when an almost identical model is used, the accuracy of the temperature between the modelled and the measured temperature is well below 10 [°C]. Since the DNO has no measurements available in terms of temperature in MV cable systems, the obtained sheath temperature within this research will probably have a similar error margin.

2.2.4. ARMOR

For a single core cable, the thermal resistance of the material between the sheath and the armour is calculated by equation 2.18. Since the XLPE cables used by the DNO do not contain an armour layer this resistance will be neglected in this research. This layer is important if the cable has an armour layer, which is the case with the examined three core PILC cable the armour loss is taken into account. Since the XLPE cable has no armour $T2$ will be zero together with the loss factor (λ_2) and the thermal capacitance Q_a.

$$T_2 = \frac{\rho}{2\pi} \ln(1 + \frac{2t_2}{D_s}) \tag{2.18}$$

2.2.5. JACKET

The jacket of a cable is its first layer of protection from the ambient material it is laid in or exposed to. The jacket of XLPE cables is mainly constructed from PE which has almost identical thermal properties as XLPE, since it is the same material but not cross-linked. To calculate the thermal resistance of the cable jacket, equation 2.19 is used.

$$T_3 = \frac{\rho}{2\pi} \ln(1 + \frac{2t_3}{D_a}) \tag{2.19}$$

In a similar fashion as the dielectric, the thermal capacitance of the jacket is allocated, this is done using Equation 2.20. The total thermal capacitance of the jacket is calculated using Equation 2.21, the volumetric specific heat of PE is similar to XLPE which is used in the insulation.

$$p' = \frac{1}{2ln(\frac{D_e}{D_s})} - \frac{1}{(\frac{D_e}{D_s})^2 - 1} \tag{2.20}$$

$$Q_j = \frac{\pi}{4}(D_e^2 - D_a^2) \cdot c_p \tag{2.21}$$

2.3. AMBIENT

Modelling the ambient in a correct way is a very important factor for the calculation of the thermal performance of underground power cables. Actually, after the conductor gauge and maybe the bonding technique, the soil thermal resistivity is the factor that limits the ampacity the most in an underground cable system [8] [10] [15]. To precisely calculate the ampacity of a cable connection it is important to know the parameters of the ambient medium very well. This can be quite challenging for long cable connections since the composition and the moisture content of the material can deviate over the whole trajectory. In order to set the ampacity of the whole connection, the most negative ground conditions should be taken. This section will form the hot spot that will limit the ampacity of the whole connection. In the Netherlands, MV cables are mostly surrounded by soil, but in some cases by sand, peat or clay. The thermal resistance of these materials differs significantly due to the different compositions and moisture content. The thermal resistivity of these materials can differ over a bandwidth. These values are available from the DNO [16]:

- Sand 0.4 - 1.5 [Km/W]
- Clay 0.5 - 1.3 [Km/W]
- Peat 1.8 - 3.0 [Km/W]

How the temperature of the soil changes is governed by a partial differential equation, with the assumption that the cable is presented by a line source located in a homogeneous infinite medium with a uniform temperature. If the partial differential equation is integrated and the remaining integral is evaluated using a series (Equation 2.22), the equation to calculate the temperature rise of the outside of the cable above the ambient temperature becomes Equation 2.23, see [17]. Which is mainly dependent on the thermal resistivity of the ground, thermal diffusivity, placement depth and total loss.

$$\begin{aligned}
&\text{for } 0 \leq x \leq 1 \\
&\qquad -Ei(-x) = -\ln(x) + \sum_{i=1}^{6} a_i x^i \\
&\text{for } 1 < x < \infty \\
&\qquad -Ei(-x) = \frac{1}{xe^x}\left(\frac{x^2 + b_1 x + b_2}{x^2 + b_3 x + b_4}\right) \\
&a = [-0.5772\ 1.0000\ -0.2499\ 0.0552\ 0.0098\ 0.0011] \\
&b = [2.3347\ 0.2506\ 3.3307\ 1.6815]
\end{aligned} \tag{2.22}$$

$$\theta_e(t) = \frac{W_l \rho_T}{4\pi}\left(-Ei\left(\frac{-D_e^2}{16t\delta}\right) - \left(-Ei\left(\frac{-L^2}{t\delta}\right)\right)\right) \tag{2.23}$$

SOIL

The thermal resistivity of soil is an important factor to determine the maximum ampacity of an underground cable. The soil thermal resistivity is a local parameter and can change over the trajectory of a cable route. The IEC60853-3-1 [18] gives an approximation for different countries on average ground conditions. For the Netherlands, the global site references are given in a table in Appendix A.

Due to the heating effect that the cable has on its surrounding, the moisture level in the ambient of the cable may vary. The moisture content in the soil has a great influence on the thermal resistivity of the soil. The resistivity will increase when the soil is dry and will decrease when the moisture content rises, resulting in different thermal behaviour of the cable buried directly in the ground [19].

This effect is also further examined in [20] where it is stated that moisture migrates away from a cable under high load leading to an increase in the surrounding soil thermal resistivity. Dry zones are formed due to the migration of moisture in the soil. This happens due to the cable losses which heat its surrounding medium. With the local migration of moisture from the soil, the thermal resistance rises, this has an influence on the ability of the soil to dissipate heat. With the increased resistivity it is even harder to dissipate the generated heat, this results in additional heating, which in its turn drives away even more moisture. Dried-out zones may form in the surrounding soil of a cable after long operation (multiple years) of high loading in underground cables. If the cable is not able to dissipate its heat properly and the cable is still nominally loaded, the cable surface temperature rises continuously resulting in a thermal runaway. If this is not prevented a thermal breakdown in cable isolation may occur. In [20], it is stated that 29% of the cable current rating might decrease when drying-out occurs. The articles performed an experimental test on three different types and samples of soil/sands, the results are in Figure 2.3.

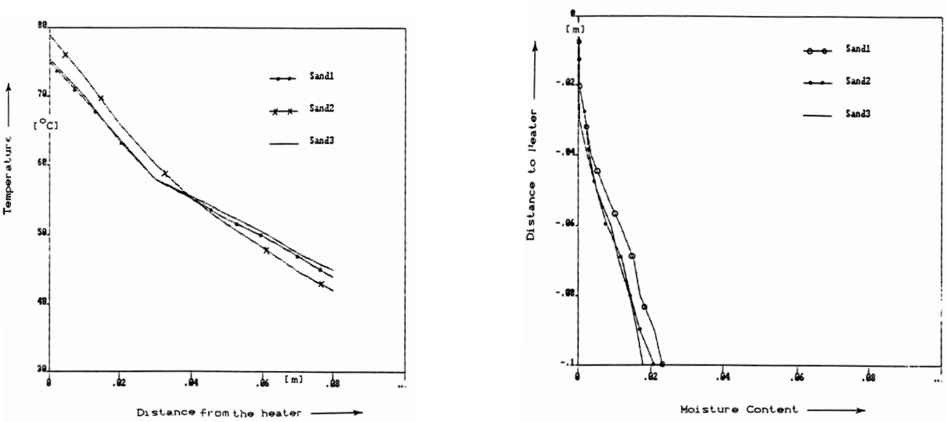

(a) Temperature versus distance for various sand types

(b) Moisture distribution at different points in sand

Figure 2.3: Moisture change in soil due to heating [20]

As seen in Figure 2.3 the phenomena of moisture migration start to happen when the cable surface reaches around 55 [°C]. This limit is an important factor in the analysis that will be performed. It could be that the outside cable temperature is the limiting factor for cable ampacity if drying out of soil should be mitigated to safeguard the ampacity over a longer period of time.

The thermal resistivity of the soil is taken to be uniform. It can be computed with the burying depth of a cable, the thermal resistivity of the soil and the external diameter of the cable, as seen in Equation 2.24.

$$T_4 = \frac{\rho_T}{2\pi} \ln\left(\frac{2L}{D_e} + \sqrt{\left(\frac{2L}{D_e}\right)^2 - 1}\right) \tag{2.24}$$

Article [14] describes a way to approximate the seasonal variation of the ground temperature which can be approached by Equation 2.25, where t is the day in the year. When analysing the ground temperature in a certain spot in the port of Antwerp over a period of three years, the authors found a simple equation that gives a good representation of the measured ground temperature of the soil in the port of Antwerpen. This temperature can be used as an offset in a dynamic temperature calculation. This estimation can be used in this research as a starting point and a bandwidth for ground temperature variation. This will only be useful for longer simulations which last longer than one day. The ground temperature variation in the port of Antwerpen as described by the equation varies between 8 and 26 [°C].

$$T = 17 - 9cos\left(\frac{t \cdot 2\pi}{365} - \frac{\pi}{5}\right) \tag{2.25}$$

The site reference in Appendix A gives a slightly different bandwidth for temperature change in the soil. It stated that the change will take place between 5 and 20 [°C]. Since the ground composition and temperature will deviate at different locations around the globe. The remainder of this thesis uses the soil temperature values of Appendix A, since they are specific for the Netherlands and no measurement data is available for the specific area of the DNO. If at a certain site the ground conditions are not sufficient to guarantee a certain ampacity for a longer duration, the DNO may decide to use other soil types as backfill. This way the first layer of material around the cables will have a lower thermal resistivity to ease the conduction of heat and benefit ampacity.

GROUNDWATER

Article [21], by a practical approach, shows that groundwater recharge plays an important role in moisture redistribution in soil, which in turn affects the soil thermal properties. Both moisture content and temperature decreased with the increase in groundwater depth. Estimating the varying soil thermal resistivity will be crucial for determining the ampacity of a certain cable track. It is very hard to analyse the effect that groundwater has on the thermal resistivity and capacitance of the ground. To simplify the groundwater variation Table 2.1 is used. In most literature, the amount of groundwater penetration is included by a factor on the thermal ground thermal resistivity and is probably empirically determined.

Groundwater in meters	2	3	4	5
Correction factor ampacity	1.10	1.04	1.00	0.99

Table 2.1: Groundwater level correction factors [22]

Groundwater levels are also a local parameter and need to be measured for specific areas and will vary over time. The correction factors can be used in specific cases by the DNO, but since the effective gain in ampacity is minimal.

3

Proposed Modelling of Cable Thermal Behaviour

When the elements of Chapter 2 are combined into a single model, two types of simulations can be studied. A steady-state thermal model where the end temperature of a certain loading can be computed and a dynamic model where the temperature can be calculated on different time instances.

The two cases of modelling:

- Steady-state
  All variables and parameters are considered to be constant and time is neglected. In a steady-state, the net temperature exchange is zero (equilibrium).

- Dynamic
  A time-varying simulation is performed, where certain parameters change over time. Time constants of the system have to be considered, this method will be further studied during this research since it gives more realistic results and is more suited for optimization studies when a load profile is applied to a component.

The different cable components are modelled and combined using the TEE model which is described in section 3.1 this deterministic analytical model is built in MATLAB (version R2020b) [23]. In order to validate the analytical thermal cable model, a Finite Element Model (FEM) of the cable is made in COMSOL Multi-physics (version 5.3.0.316) [24]. The cable is constructed in a "Heat Transfer in Solids (ht)" model. The FEM model is also used to calculate the temperature response of a MV cable when a load profile is applied. The same material-specific parameters are used. An overview of the input/output and data flows for both simulations is given in Figure 3.1. This chapter will give an overview of how both models are constructed and the used assumptions.

3

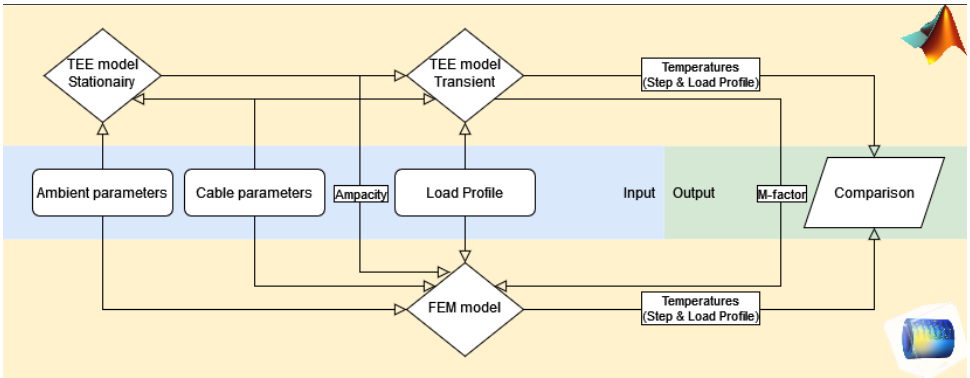

Figure 3.1: Illustration of the models

3.1. ELECTRICAL EQUIVALENT THERMAL MODEL

To determine the dynamic temperature response of a cable when a step or load profile is applied, an enhanced lumped parameter model could be used, which is also known as Thermo Electric Equivalents (TEE) [25]. A simplified TEE model of an unarmoured cable with the metallic and semi-conductive layers neglected is shown in Figure 3.2. All the thermal resistance, capacitance and heat elements are included in this single model. For stationary simulations, it can even be further simplified and the thermal capacitance can be neglected.

To calculate the transient thermal response of the system, the temperature rise is calculated in steps. Firstly the temperature rise of the conductor is calculated using the cable parameters and the applied current, the temperature rise at time instant t can be calculated using the short-circuited ladder circuit shown in (b) of Figure 3.2. Where the two heat sources (conductor and screen) and all the thermal resistances and thermal capacitance of the different layers in a cable are taken into account. The thermal resistances of all the metal parts in a cable have a small contribution since they have almost no contribution to the total heat transfer. This is due to the fact that thermal resistance is the inverse of thermal conductance. The thermal conductance of metal is rather high compared to the other layers inside the model, resulting in a very low thermal resistance. Equation 3.1 shows how the components are grouped to form the two-looped thermal network in Figure 3.2 (c).

$$T_A = T_1 \quad T_B = (1+\lambda_1)T_3 \quad Q_A = Q_c + pQ_i \quad Q_B = (1-p)Q_i + \frac{Q_s + p'Q_j}{1+\lambda_1} \tag{3.1}$$

Secondly, the attainment factor (α, Eq. 3.2) is calculated to account for the transient temperature rise between the conductor and the outside surface of the cable. The attainment factor can be derived from the ratio between the transient conductor temperature at instant t and the steady state temperature of the conductor above the outside cable temperature.

To fully calculate the transient temperature rise of the conductor above the ambient

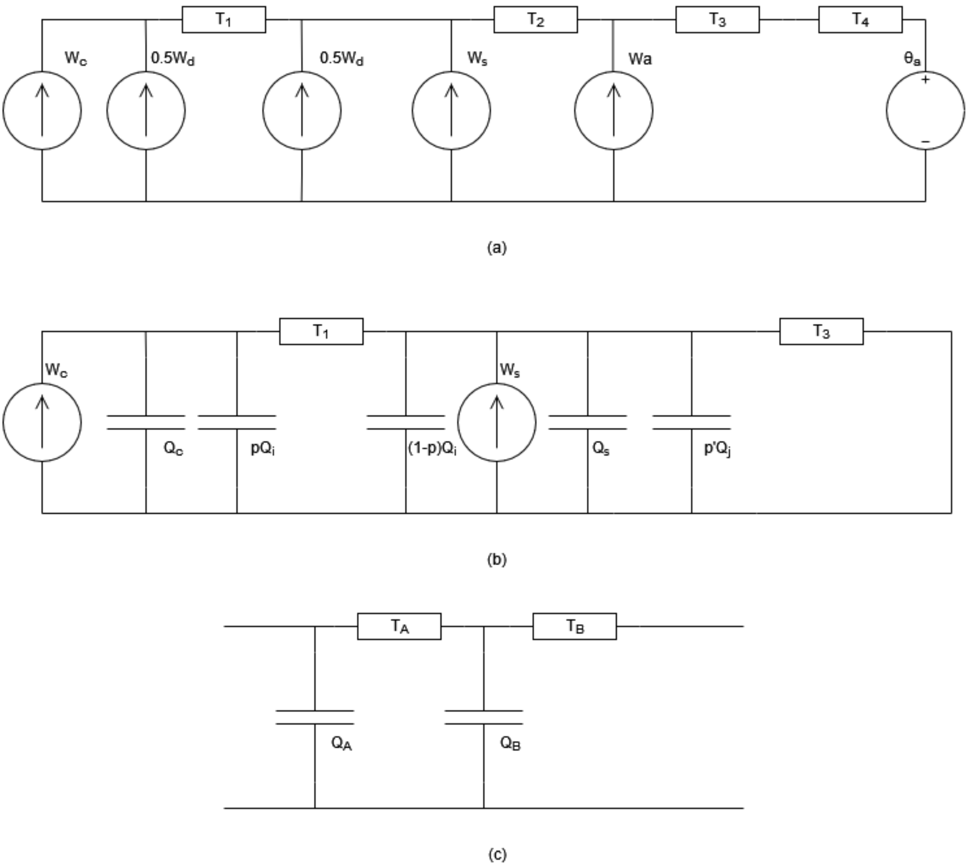

Figure 3.2: Decomposition of TEE circuit, (a) single core cable, (b) long duration transient single core unarmoured cable and (c) equivalent network transient response

temperature, the temperature rise of the conductor above the outer surface of the cable must be added together with the temperature rise of the outer surface of the cable above ambient temperature, Equation 3.3. To obtain the operating temperature of the conductor the ambient temperature must be added to the result of the temperature rise above ambient (Equation 3.4).

$$\alpha(t) = \frac{\theta_c(t)}{W_c(T_A + T_B)} \tag{3.2}$$

$$\Delta\theta(t) = \theta_c(t) + \alpha(t)\theta_e(t) \tag{3.3}$$

$$\theta(t) = \theta_c(t) + \alpha(t)\theta_e(t) + \theta_a \tag{3.4}$$

3.2. STATIONARY (IEC60287)

A continuous nominal load which is time-independent is applied in the stationary loading calculation of components. Due to the absence of time in the calculation, the equations are greatly simplified. All the thermal capacitances can be neglected and only thermal resistances and losses need to be calculated to obtain the ampacity based on the thermal limits of the cable. To calculate the stationary current rating of an underground cable Equation 3.8 is considered where the cable is not influenced by solar radiation, drying-out of soil does not occur and the soil surrounding the cable is homogeneous with a constant thermal resistance. When $W_c = I^2 \cdot R$ is considered the steady state current can be calculated. Using the fact that the total Joule loss is the summation of the conductor loss, sheath loss and armour loss (Equation 3.5). The temperature rise of the conductor above ambient temperature is then calculated using Equation 2.3 & 3.6, derived from 3.2 (a).

$$W_l = W_c + W_s + W_a \Rightarrow W_c(1+\lambda_1+\lambda_2) \tag{3.5}$$

$$\Delta\theta = (W_c + 0.5W_d)T_1 + (W_c(1+\lambda_1)+W_d)nT_2 + (W_c(1+\lambda_1+\lambda_2)+W_d)n(T_3+T_4) \tag{3.6}$$

The temperature rise above ambient temperature due to the dielectric loss should be subtracted from the total temperature rise, since this is independent of the current but does add extra loss and thus heat which has to be incorporated.

$$W = \frac{\Delta\theta}{T}; \quad I = \sqrt{\frac{W}{R}} \quad \Rightarrow \quad I = \sqrt{\frac{\Delta\theta}{TR}} \tag{3.7}$$

$$I = \sqrt{\frac{\Delta\theta - W_d(0.5T_1 + n(T_2+T_3+T_4))}{RT_1 + nR(1+\lambda_1)T_2 + nR(1+\lambda_1+\lambda_2)(T_3+T_4)}} \tag{3.8}$$

When partial drying-out of the soil occurs Equation 3.9 needs to be used since it takes a two-zone approximation where a zone adjacent to the cable is dried out whilst the zone around this shell remains at a lower thermal resistance. In the equation factor v stands for the ratio of the thermal resistivity of the dry-zone divided by the wet zone ($v = \rho_d/\rho_w$).

$$I = \sqrt{\frac{\Delta\theta - Wd(0.5T_1 + n(T_2+T_3+vT_4)) + (v-1)\Delta\theta_x}{RT_1 + nR(1+\lambda_1)T_2 + nR(1+\lambda_1+\lambda_2)(T_3+vT_4)}} \tag{3.9}$$

The resulting current in Equation 3.8 or 3.9 is the ampacity of the cable with the given maximum temperature increase of the conductor above ambient temperature ($\Delta\theta$) with the given ambient and cable parameters.

3.3. DYNAMIC/TRANSIENT (IEC60853)

The temperature of a cable fluctuates under varying load conditions, for instance when a cyclic load is applied. A dynamic thermal rating of a cable is needed when in search of momentary or long-term maximum cable exploitation. It is assumed that the voltage on the cable is applied long enough that the dielectric loss of the cable has reached a steady state and only the loss due to the current passing through the cable is varying. The total temperature rise of the conductor above ambient temperature is the sum of the steady-state dielectric loss temperature rise and the transient temperature rise due to the loss of the changing current. These varying losses include the conductor and the induced sheath loss.

The method that is still used in a vast majority of studies and software packages is the Neher-McGrath method [5] [19]. This method was introduced in 1957 and gives a very detailed approach how to calculate the temperature rise and loading capabilities of cables and forms a basis for the IEC 60853.

From the two-looped network in Figure 3.2 (c) a transfer function is derived in the IEC60853 [17]. Using this function the temperature response of the conductor and sheath above ambient temperature is computed. This research focuses on these two temperatures which make this approach a good fit. The derivation of the transfer function can be found in the IEC60853 [17]. The formulas for the resulting coefficients are given below, they show how the different grouped thermal resistances and capacitance determine the temperature response. To obtain the time-dependent temperature response of the conductor above the outer temperature of the cable, coefficients a, b, T_a, T_b, M_o and N_o must be determined, see Equations 3.10, 3.11 and 3.12.

$$M_o = \frac{1}{2}(Q_A(T_A + T_B) + Q_B T_B) \qquad N_o = Q_A T_A Q_B T_B \tag{3.10}$$

$$a = \frac{M_o + \sqrt{M_o^2 - N_o}}{N_o} \qquad b = \frac{M_o - \sqrt{M_o^2 - N_o}}{N_o} \tag{3.11}$$

$$T_a = \frac{1}{a-b}(\frac{1}{Q_A} - b(T_A + T_B)) \qquad T_b = T_A + T_B - T_a \tag{3.12}$$

The resulting formula which uses the coefficients to obtain the temperature rise of the conductor above the outer surface of the cable temperature is given in Equation 3.13. Together with Equation 3.3 the total temperature rise of the conductor above ambient temperature can be calculated.

$$\theta_c(t) = W_c(T_a(1 - e^{-at}) + T_b(1 - e^{-bt})) \tag{3.13}$$

3.3.1. M-FACTOR

When a cyclic load profile is applied on a MV cable, the components inside the cable have moments of lesser loading where it has the ability to transfer some of the heat that has been accumulated due to losses to the surrounding medium (energy balance, see section 2.7). This effect of moments of less loading in the load profile has a positive impact on the overall temperature of the component during a load profile cycle when it is compared to a continuous load with the same magnitude as the peak of the load profile.

If the same reoccurring 24-hour load profile has been applied long enough that an energy balance has been reached. The average temperature during a 24 hours load cycle will be almost equal to the end temperature when a step load is applied with the average load factor of the load profile. The peaks of the load profile will be higher than the continuous loading but this will be compensated by the moments of lesser loading in the load profile. Due to the thermal capacitance in the different layers of the MV cable, temperature built-up takes time, this enables the possibility of momentarily overloading the cable above nominal ampacity, this can only be achieved if this is compensated by moments of lesser loading inside the cyclic load profile.

When a load cycle of 24 hours is recurring over a longer period of time the overload factor/ cyclic rating factor (M-factor) can be calculated by using the cable parameters calculated in Chapter 3. This method gives a factor by which the whole recurring 24-hour load profile may be multiplied so that the peak of the profile exceeds the nominal ampacity rating of the cable. The peak of the load profile exceeds the nominal ampacity of the cable with this factor and the thermal limits of the cable or the ambient (soil dehydrating) are not exceeded. The M-factor is only dependent on the shape of the profile and is independent of the actual magnitude of the current. For a known load profile this gives the DNO the ability to load their cables structurally above the nameplate rating.

The factor can be calculated by using the method described in the IEC60853 [17]. A 24-hour load profile should be decomposed into hourly load pulses and divided by the nominal ampacity to obtain a ratio of the maximum current. These hourly pulses are squared to get hourly ordinates ($Y_i \to [Y_0 - Y_{23}]$) of the load profile, this is done to take Joule losses into account.

The average temperature at the equilibrium of the profile is determined by the loss-load factor (μ, Equation 3.14) of the load profile. On top of this, the temperatures of the hourly pulses of the six hours prior to the expected highest temperature inside the load profile are summed. The time between the rectangular pulse prior to the maximum temperature and the time constant of the system is also taken into account. This is done by using the temperature ratio of the first six hours divided by the steady-state temperature of the step response of the system. The temperature difference of the first six-hour steps of the step response is taken as guidance for the temperature accumulation towards the peak of the profile above the average temperature (Equation 3.15). How $\frac{\theta_R(i)}{\theta_R(\infty)}$ is computed can be found in Appendix B, where i is the time from the start of the simulation in hours.

$$\mu = \frac{1}{24}\sum_{i=0}^{23} Y_i \tag{3.14}$$

$$M = \frac{1}{\sqrt{\mu\left(1-\frac{\theta_R(6)}{\theta_R(\infty)}\right)+\sum_{i=0}^{5} Y_i\left(\frac{\theta_R(i+1)}{\theta_R(\infty)}-\frac{\theta_R(i)}{\theta_R(\infty)}\right)}} \tag{3.15}$$

The method in the standard describes that the expected highest temperature peak in the load profile should be picked by visual inspection and the six hours prior to this should be taken. This is prone to mistakes and requires manual labour for each different load profile. To automate this process the M-factor is determined 24 times for each load profile. The smallest M-factor is picked from the range, and this will be the limiting M-factor for the whole load profile.

3.4. FINITE ELEMENT MODEL

A FEM is constructed by using the same parameters as used in the analytical model. The geometry of the cables in trefoil formation is constructed in a "Heat Transfer in Solids" model. Surrounding this geometry the soil is modelled by using a big rectangle, big enough to hold the temperature gradient towards the boundaries at maximum ampacity. To calculate the temperature in the model the geometry is divided up into a large number of small triangles, so-called finite elements forming a mesh. Within these triangles, the PDEs are computed with their boundary conditions, if the solution converges and is smaller than the specified convergences error the next triangle is calculated. This is done for every time step in the simulation. To increase accuracy the mesh could be made finer and the convergence error smaller, this has a downside which also increases computation time. This method requires more computational power and time to solve than the analytical model presented.

The results of this model are used to validate the results of the analytical model and to gain deeper insight into the temperature response of a load profile. An overview of the geometry of the model is given in Figure 5.3. The used dimensions and material properties are given in Appendix C, and the used current rating is obtained from the analytical model (Section 3.2).

3.5. PRESENCE OF MEASUREMENTS & ASSUMPTIONS

The best practice is to validate the model on measurements that are installed in the field for a longer period of time to also take seasonal variation into consideration. Since there are currently no measurements of the conductor nor sheath temperature being taken by the DNO, the model can not be validated using this data.

There is no current or up-to-date map of the ground thermal resistivity available at the DNO to narrow down the bandwidth of this parameter during this research. So as stated the bandwidth specified in the site conditions of Appendix A will be used.

Since the available data is very limited and every MV connection is unique, assumptions have to be made. Every model needs a certain set of assumptions if data is unavailable and a scope to define borders. It is best to keep the assumptions to a minimum in order to stay as close to reality as possible. The following set of assumptions is made during this research:

- The surrounding medium of a MV cables is taken to be uniform, e.g. pockets of fluids like groundwater are not being considered
- The cable is buried one meter below the surface along the whole length of the cable

trajectory

- The cable is energized long before simulations are started so that the dielectric loss is constant
- Heat will not travel in the direction of the cable, since the same amount of heat is generated in the next 2D slice of the cable
- Three single-core cables are laid in a perfect Trefoil formation
- With a sheath temperature of 45° Celsius drying-out of soil can not occur
- Skin and proximity effects are neglected
- The bandwidth of the ambient parameters given in Appendix A comply for the whole area of the DNO.
- The underground MV cable is not placed in a pipe or duct
- No other heat sources are present nearby the MV cable

4

Load Profile & Simulation Approach

To analyse how the thermal behaviour of cables in the ground changes under dynamic load conditions, different scenarios are constructed. How the shape of the aggregated load profile is going to change in time is uncertain. Different aggregated load profiles are created using a significant number of LV load profiles as their basis. Aggregated load profiles can be used since the number of LV connections is rather high, these connections are connected through MV/LV transformers to the MV ring topology. To emphasise the urgent need for this research some background on the growth of EV and PV systems is given, as to how the different load profiles for the case studies are formed. Some base load profiles are created and scaled and summed to obtain new load profiles which can be used in the case studies.

4.1. Electric Vehicles

Since there is an urgent need to limit our oil use and carbon emission, more electric vehicles are being produced and used in the Netherlands. The prediction of the number of electric vehicles in the Netherlands by ElaadNL is given in Table 4.1. It clearly shows the expected growth of EVs in the Netherlands. It is important to know the impact that this extra load will have on the MV network.

The rapid rise of EVs creates challenges for the electricity network in terms of the

Prognosis ElaadNL e-mobility			
	2021	2035	2050
EVs [no. vehicles]	400.000	4.058.800	9.112.800
EVs [%]	3.4	44.5	98.6

Table 4.1: Outlook ElaadNL Q3 2021 growth of EVs in the Netherlands [2]

power demand to charge all these vehicles. When no smart charging algorithms are applied all EVs will start to charge whenever the user plugs their car into the grid. The moment when most of the users do so is coinciding with the moment when people come home and start using electricity in their homes. The problem of the coinciding charge of electric vehicles and residential daily load profile is visualized and analysed in Article [26]. The histogram in Figure 4.1 shows the (minimal) spread during a normal working day when an electric vehicle arrives at home to be charged. The power demand of these EVs can be spread over the night when smart charging is introduced. The goal of smart charging is to limit the peak demand and spread the energy demand so that the peak power demand is limited. Shifting power or also called peak shaving to other moments of the day changes the shape of the load profile which has an effect on the thermal behaviour of the MV cable during recurring load profile cycles, this is further explained in section 5.4.

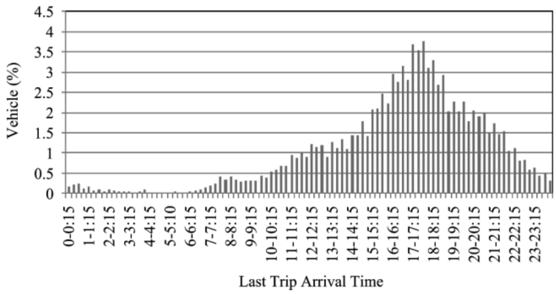

Figure 4.1: Percentage of vehicles versus their home arrival time for the weekdays of summer. [26]

The problem of the high simultaneity of EVs and residential load does not end at the borders of the Netherlands, in [27] the concern is further analysed for the UK grid. The move to plug-in vehicles will destabilize the electricity system, due to the increased burden of charging EVs, especially during peak load hours. To tackle this problem a lot of novel concepts are being engineered. One of the solutions provided is smart charging regimes, a conceptual diagram of such a solution is shown in Figure 4.2. Load shifting will come with some benefits and drawbacks. The benefit will be that the load peaks of residential loads will not coincide with the charging of EVs, this technique will utilize the existing components more, which can postpone investments. A drawback which will be further analysed within this research is the continuous loading (24/7 at a certain load factor) of components. When continuous loading is applied to components there is no time window in which it is able to cool down. This will result in not having the ability to structurally overload components with a certain cyclic load profile.

The profile for controlled EV charge in Figure 4.4 is an expected load profile for smart charging. The aim is to shift as much of the energy to moments where there is less power demand, but keep a certain base load for cars that do not offer flexibility. The profile for the controlled charge of EVs will be dependent on the controller or aggregator which controls the set of charging stations or EVs and the amount of congestion at that given moment. For this research, a load profile for EVs is constructed from a data set which

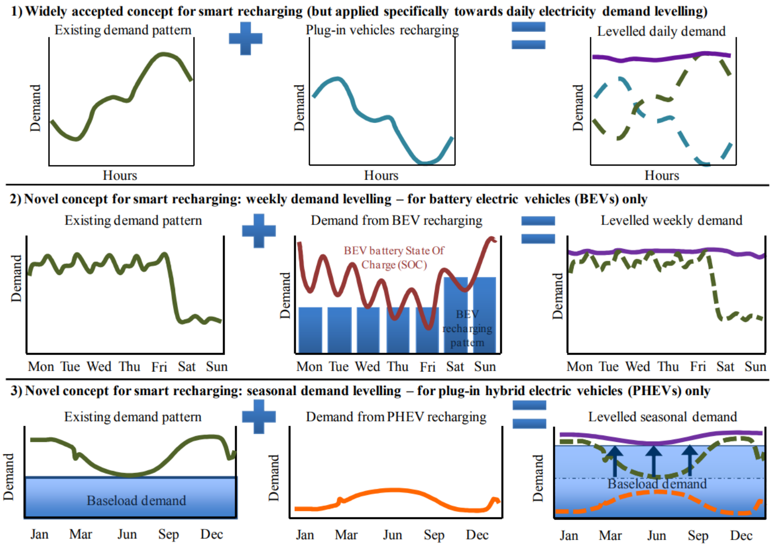

Figure 4.2: Concept diagrams for smart recharging (daily, weekly, seasonal) [27]

contains about 170,000 charge transactions in the Netherlands (Elaad NL [28]) from the period of 2015-2016. The load profile is given in Figure 4.4 and is used to obtain different case studies with different amounts of EVs. The same scaling factor as uncontrolled charging of EVs will be used as stated in the introduction of this chapter, to have an equal amount of energy.

4.2. PHOTO VOLTAIC SYSTEMS

The amount of generated PV power of a single system is mainly dependent on temperature, solar irradiance and orientation. These three factors differ per area across the Netherlands. Since this study focuses on MV cables the number of connected PV installations is significantly high. Since this number is high there is a good mix of the three factors mentioned earlier, hereby an aggregated load profile of PV suffices.

An aggregated load profile is taken from MFFBAS [29] and the peak in the profile during the summer is taken to be 100%, during the winter there is less solar irradiance (Figure 4.3) but also a decrease in ambient temperature which is beneficial for the cable ampacity. The profile of winter PV is scaled with the same factor as the summer PV profile, this results in a winter PV peak of the aggregated profile that is limited to around 55% of the summer peak. Since PV generation only happens during the daytime when there is solar irradiance the simultaneity of solar power is pretty high.

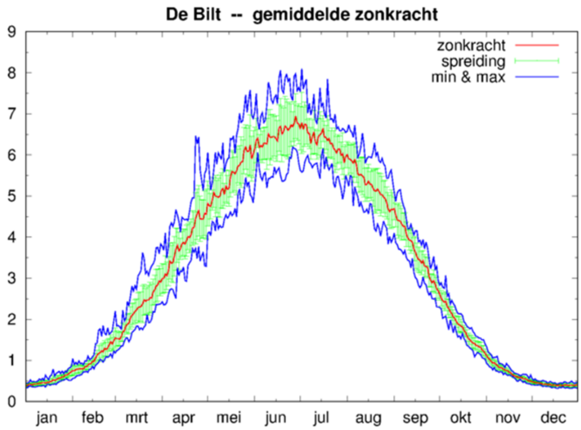

Figure 4.3: Average sun-power 2018 UV index (De Bilt, the Netherlands) [30]

4.3. LOAD PROFILES

Since the current penetration of PV systems and EVs is still rather low the current aggregated household load profile can be taken as a base. The aggregated daily load profiles of households and PV are taken from MFFBAS [29] (formally known as NEDU). The aggregated load profile of EV is from ElaadNL [28] and a load profile for smart charging is created by filling the gaps in the household profile during the night. The controlled charging load profile is arbitrary and dependent on an aggregator or system, for this research it is not important how and when the load profile is going to change but what the impact will be of these changes. To develop the used load profiles certain assumptions are made to come to new load profiles of the MV grid. All the used profile types are scaled to unity on their peak value before any computation is done, and the seasonal difference in peak value is preserved. To give an estimation of the different levels of peak demand that the different profiles have. Key numbers for simultaneous power of different demands on MV/LV transformer level that the DNO uses are given below. These factors will also be used to scale the different load profiles to create case studies.

- Household consumption = 1.5kW
- Charging of EV (controlled and uncontrolled) = 1.5kW
- PV generation = 4kW

To analyse the result of changing load profiles on MV cables, different 24-hour load profiles are examined. By using the hourly aggregated profiles (Figure 4.4) and the scaling factors for the different load profiles stated above, profiles are created that consider additional PV systems and EVs in the network. Household demand is always kept at a constant level (100%) and the amount of PV and EV is varied in steps of 0, 25, 35, 50, 75 and 100% and summed to create different load profiles that could occur on MV cable connections. This creates different stages of extra burden due to PV and EV on the network. The seasonal effect is taken into consideration by using summer and winter

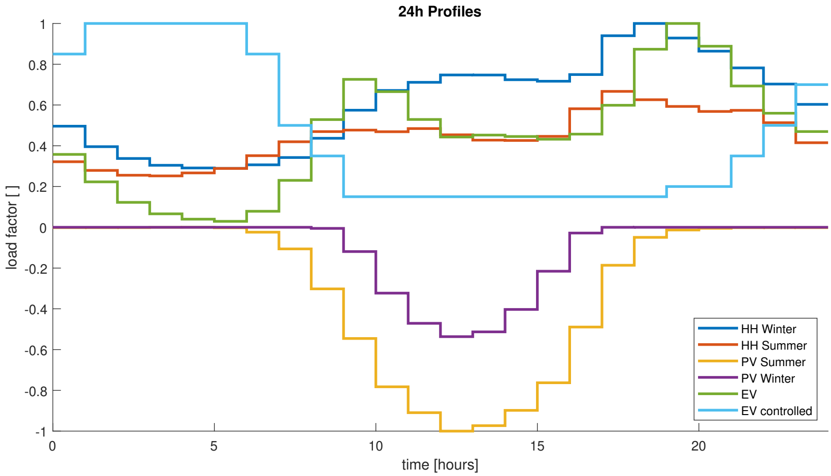

Figure 4.4: Hourly aggregated load profiles for different types of demand or generation

profiles. The effect that these case studies have on the ampacity of MV cables is calculated in Section 5.3. The different case studies are also hourly based but to ease readability a line graph is presented for the different case studies. All the case studies are compared with a profile that contains a constant nominal loading at the rated ampacity over 24 hours (step load). The case studies should provide insight into how the shape of the profile affects the overloading/ cyclic rating capabilities of a MV cable connection, and how the thermal room is represented in the load profile. Care should be taken when the shape of the load profile changes if the overload capabilities can be retained, altered or discontinued.

5

Simulations & Analysis of the Results

Steady-state simulations are conducted to obtain the nominal ampacity value of a MV cable. Transient simulations are computed to study the temperature response, with a certain set of input parameters. The effect that these input parameters have on the output of the system is studied. Due to missing measurements and data, sensitivity analyses are done to see the impact of each parameter and the potential gain of field measurements.

A comparison is made between the analytical and the finite element model, to validate the obtained temperature response of the analytical model. The results of the different case studies are being studied, to see the impact that a changing load profile has on the ampacity and a theoretical example of MV cable loading is simulated.

5.1. Simulations

As stated in Chapter 3, two kinds of simulations are done. Firstly, stationary to compute the nominal loading of a MV cable and secondly a dynamic study to compute the overloading capabilities for a certain recurring load profile. To validate the analytical model a FEM model is constructed using the same XLPE cable. Additionally, a longer run-time with a load profile will be performed using the FEM model to simulate maintenance or fault events.

5.1.1. Steady-state response (step load)

The IEC60287 is used to calculate the nominal current value of different cables under different conditions. Using this approach the nominal current rating of a MV cable can be calculated when a nominal step load is applied. The maximum current rating of XLPE cables is limited by the conductor temperature or sheath temperature. This limit is dependent on the ambient and if ground dehydration is taken into consideration or not. If this is not the case and ground dehydration can not occur or is not relevant the maximum ampacity of the XPLE cable is limited by the conductor temperature which can not exceed 90 [°C]. If ground dehydration is directive for the maximum ampacity the sheath temperature may not exceed 45 [°C]. For PILC cables this is not the case since by design the conductor temperature may not exceed 43 [°C] [31]. This will result in a sheath temperature which will always be lower than 43 [°C] if the maximum current rating is not exceeded and no other heat sources are present in the neighbourhood of the cable. In this case, the sheath temperature will never exceed 45 [°C] since there is a negative temperature gradient of temperature from the conductor radially outwards.

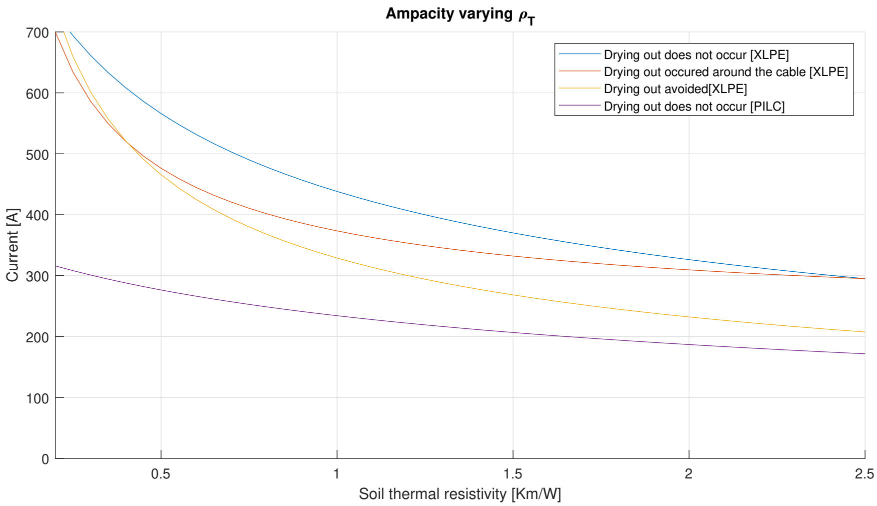

Figure 5.1: Ampacity of 3x1x240AL XLPE Trefoil and 1x3x120CU PILC for a changing soil thermal resistivity

Figure 5.1 shows the ampacity rating of the MV cable if a nominal continuous current is applied to the cable. The thermal resistivity of the material surrounding the cable is altered to see the impact on the nominal ampacity of the MV cable. For PILC cables the reference ampacity is 280[A] at ρ_T=0.5[Km/W] and for XLPE 380[A] at ρ_T=0.75[Km/W]. These reference values are also the nominal ampacity values which are widely used by the DNO. If the current values are divided by the reference ampacity rating which is used, a reduction factor for different soil thermal sensitivities can be computed for continuous loading of power cables (Figure 5.2).

This shows that if the DNO does not incorporate a validated field measurement of the medium surrounding the power cable and uses a standard ampacity for certain cables based on the references stated above. The DNO might structurally overload their cables. For instance, if a patch of ground has a thermal resistivity of ρ_T=1.5[Km/W] the ampacity for a continuous load at nominal current rating should be reduced for a PILC cable by about 25% and for a XLPE cable by about 30%. This measure needs to be taken to avoid a thermal meltdown of the materials or prevent soil dehydration.

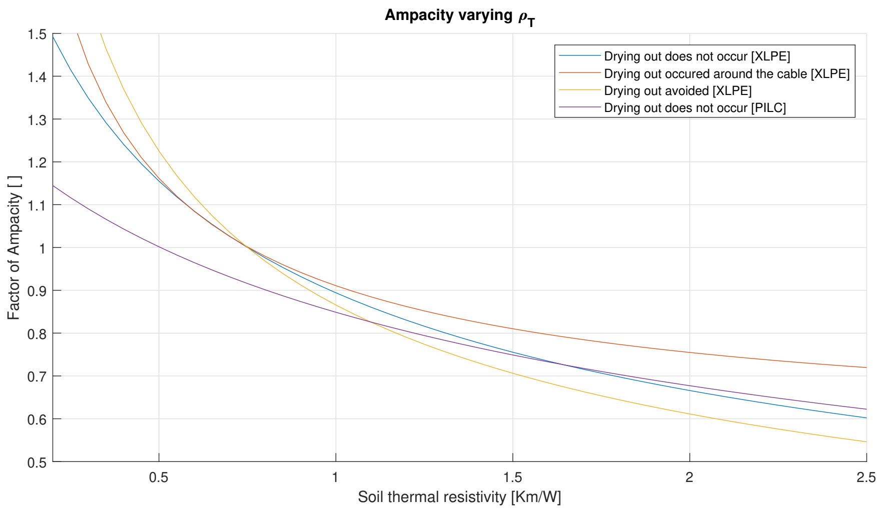

Figure 5.2: Factor of Ampacity of Figure 5.1

To validate the analytical model, a FEM model of the same XLPE cable is made in COMSOL Multiphysics. These two methods differ in their way of computing the maximum temperature and ampacity of a cable. FEM (Section 3.4) is a method for solving numerical partial differential equations (PDEs), and fits the purpose of heat transfer really well. To visualize the results from the calculated ampacity from the analytical model three current values are taken when the soil thermal resistivity is $\rho_T = 0.75[Km/W]$, and the thermal response is calculated using COMSOL. The three current values are taken from the analytical model, which has its results in Figure 5.1.

In Figure 5.3 the results are visualised, in the case where drying out of the soil should be avoided (Figure 5.3a) a maximum continuous current of 380 [A] can pass through the cable. The temperature of the sheath neatly just stays below 45 [°C], to prevent soil dehydration. The conductor can reach a higher temperature since it is not in contact with its surroundings and there is a temperature decrease from the conductor towards the sheath of the cable. In the case where drying out of the soil can not occur or will be accepted the maximum continuous current through this cable configuration is 490 [A]. The limiting factor, in this case, will be the conductor temperature which may not exceed 90 [°C], the results of this simulation in COMSOL are plotted in Figure 5.3b. If drying-out of the soil ($\rho_T = 2.5[Km/W]$, Appendix A) occurred the surface area by which the heat can spread is bigger. Since the soil surrounding the cable has already dried out the outer diameter of the dried-out zone will form the new thermal limit of 45 [°C]. This will increase the ampacity of the connection slightly from 380 [A] to 410 [A], see Figure 5.3c. If the dry-zone is too large the conductor temperature will again be the limiting factor for calculating the ampacity of the MV cable. The temperatures are slightly higher than permitted, this is due to the difference in the FEM and analytical model, see section 5.2).

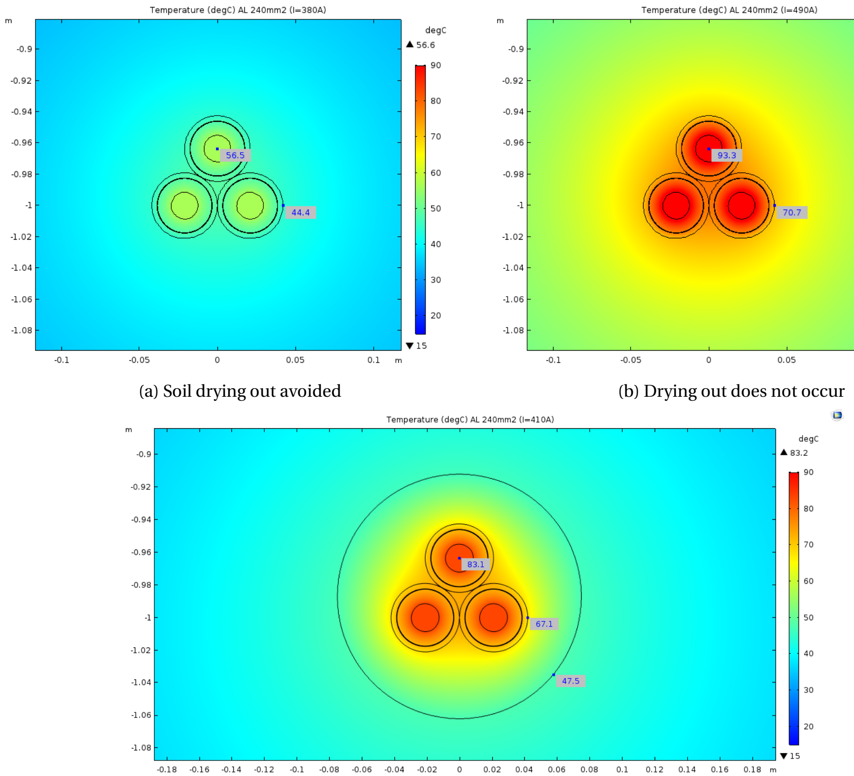

(a) Soil drying out avoided

(b) Drying out does not occur

(c) Drying out occurred (ρ_T (dry-zone)=2.5[Km/W], r=7.5[cm]

Figure 5.3: Thermal response 3x1x240mm2 AL trefoil ($\rho_T = 0.75 Km/W$)

5.1.2. DYNAMIC RESPONSE

When looking at the dynamic response of a cable when the cable loading is changed according to a step function to reach nominal loading in Figure 5.4. If only the first 30 minutes of the temperature response are being analysed, the temperature propagation can be studied. The conductor temperature will rise immediately after a current is applied. The temperature in the sheath will change at a slower pace, to further examine this change the derivative of both temperatures is taken. The rate of rise for the conductor is significantly higher than for the sheath and happens closer to $t = 0$. This delay is due to the fact that each layer has its own heat capacity, so it takes time for the heat to travel radially outwards through the different layers towards the sheath and eventually the soil. This can also be observed the temperature of the sheath stays close to the ambient temperature for the first calculation time steps after $t = 0$. This is due to the thermal capacitance of the different layers inside the cable, which need to warm up to have a temperature difference and transfer in their turn the heat further outwards.

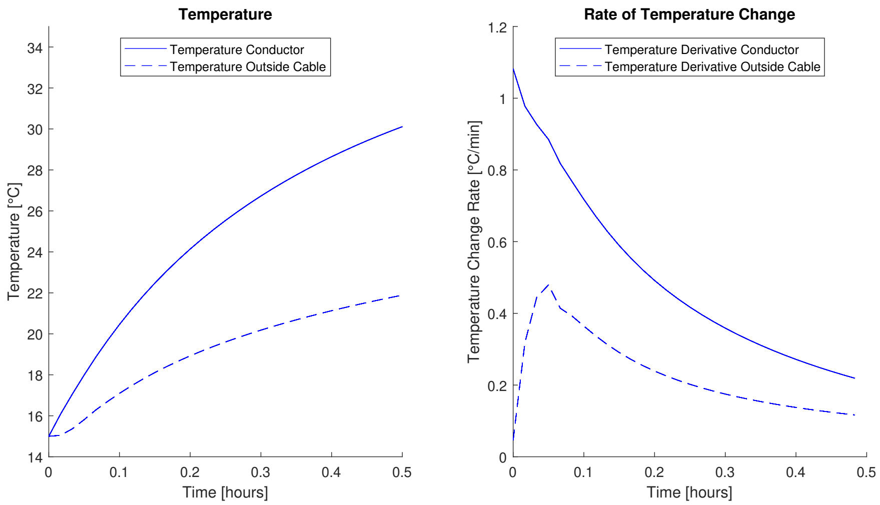

Figure 5.4: Temperature and its derivative response for nominally loaded cable

5.2. COMPARISON (ANALYTICAL & FEM)

The analytical and FEM method differ in their way of computing the temperature response of the underground MV cable. The resulting transient temperature response of the conductor and sheath temperature will be compared, to validate the simplifications in the analytical model.

The difference in the transient temperature response of the conductor and sheath temperature is visualised in Figure 5.5 & 5.6 over a period of 30 days. The difference between the temperatures of the models is also plotted in red. Both models are excited using the nominal continuous current in the first case of 380 [A] and secondly with 490 [A]. In the first case, the sheath should attain 45 [°C] and in the second case the conductor temperature must not exceed 90 [°C].

At the beginning of the simulation, the difference between the two models is the greatest peaking at a value of 4.5 and 9.5 [°C] respectively. This is due to the slope being the steepest at the beginning of the response, so any small deviations will result in the most significant error.

The difference in conductor and sheath temperature above ambient temperature at t=720 [hours] is given in table 5.1 together with the percentage difference (temperature) of the analytical model compared to the FEM model. It shows that the temperature at both current ratings deviates in a similar manner and that the temperature of the analytical model and especially the sheath temperature is higher than the more detailed FEM model. This can result in a slight underestimation of the MV cable connection if the analytical model is used. For the 490 [A] simulation where the conductor temperature is the limiting factor, this results in a reduction of the cable ampacity of about 2.7 % and for the 380 [A] simulation where the outside temperature should be matched it results in an underestimation of about 6.6 %. The difference between the two percentages is due to

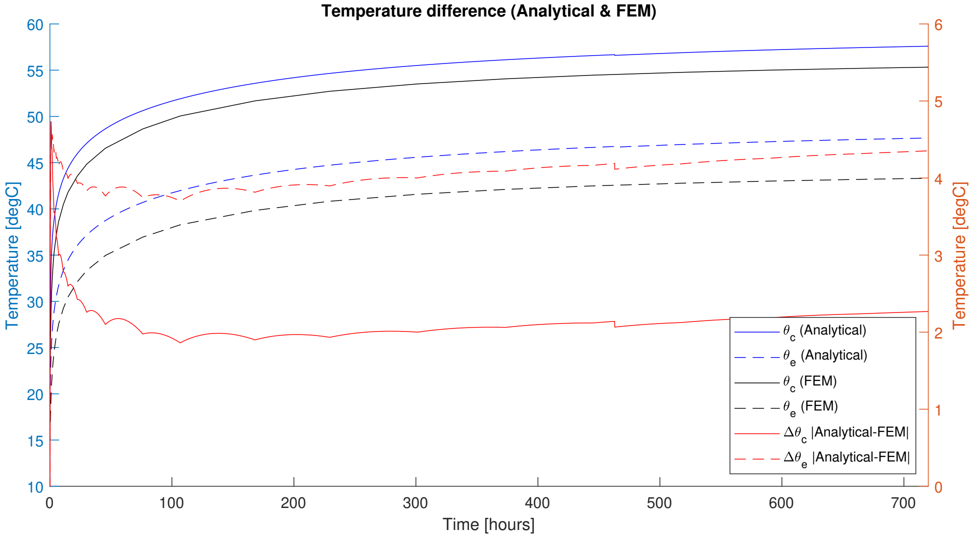

Figure 5.5: Temperature response TKF 240AL 3x1x240AL trefoil I = 380[A]

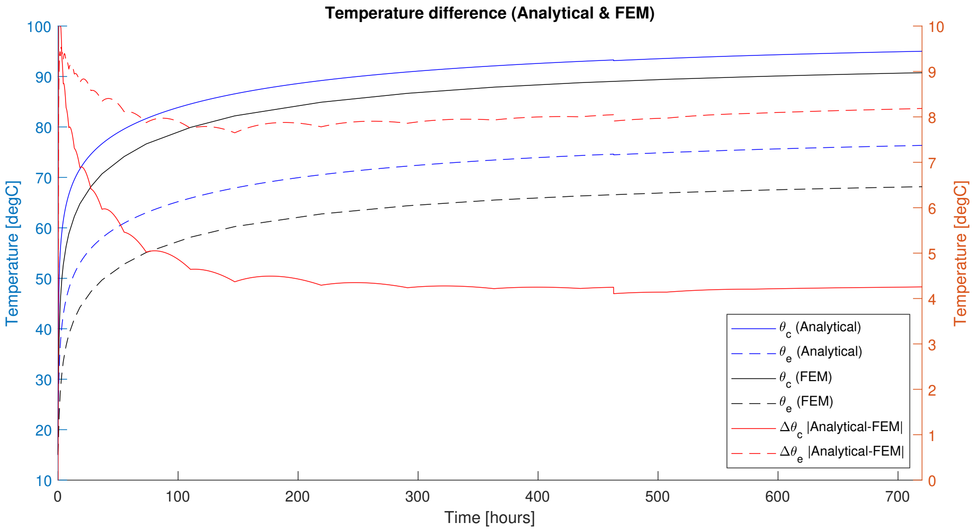

Figure 5.6: Temperature response TKF 240AL 3x1x240AL trefoil I = 490[A]

the higher deviation of the sheath temperature compared to the conductor temperature between the two models.

The error is introduced due to the conductor and sheath AC resistance being constant over their temperature range in the analytical model, where the FEM model reevaluates this value every time step. This creates higher Joule losses in the conductor and the sheath at lower temperatures. Another factor that plays a role is the neglected temperature gradient inside each layer in the analytical model. The temperature within each layer of the analytical mode is taken to be spatially uniform, so there is no internal temperature gradient at any moment in time. This will result in a different transient thermal response between the analytical and the FEM model. This can be observed in the first 200 hours of the simulation. Due to the absence of measurement data the model can not be validated using measurements.

	380 [A]		490 [A]	
	$\Delta\theta$ [°C]	[%]	$\Delta\theta$ [°C]	[%]
Conductor temperature	2.3	4.1	4.3	4.7
Sheath temperature	4.4	10.2	8.2	12.0

Table 5.1: Difference of the temperature in the analytical and FEM model

5.3. Case Studies

5

Working out the load profiles as described in Section 4.3, will give different case studies to see the impact that a changing cyclic load profile has on the overloading capabilities of a MV cable connection. All the case studies (1-24) are being compared with a traditional aggregated load profile (winter and summer) of a residential neighbourhood without the presence of DER. These two load profiles also form the base of the profile before extra load or generation is added in the form of PV and EV. On top of these household load profiles PV during the summer (case studies 1-6), PV during the winter (case study 7-12), charging of EV (case studies 13-18), controlled charging of EV (case studies 19-24) are added to see their impact on the shape of the aggregated load profile. All the resulting M-factors for the case studies are given in tables. The case studies are constructed using a summation of discrete hourly-based profiles, to ease readability a line plot is constructed of the obtained hourly load profiles. The M-factor is calculated by using a ground thermal resistivity of 0.75 [Km/W], a burying depth of 1000 [mm] and an ambient temperature of 15 [°C] for both XLPE and PILC cables.

The minimal value of the M-factor is one, this is due to the fact that when a constant nominal load is applied on the cable there are no moments of lesser loading to potentially release some of the extra accumulated heat. Resulting in not having the ability to overload the nominal ampacity structurally. With smart algorithms and price incentives, aggregators and grid operators are trying to limit congestion by shifting demand to moments of lesser loading. In best practice, this can lead to a load profile which will tend to be very similar to a constant loading at nominal ampacity for 24 hours. This will result in reducing the ability to overload a cable connection structurally. This result is seen in Figure 5.10 and Table 5.5, where charging of EV is introduced during moments of less loading. This will result in a more flattened load profile, reducing the thermal room of the load profile. In Table 5.5 the M-factor for both cable types can be seen dropping when the valleys inside the load profiles are removed. This counterparts for the positive effects that smart charging or load shifting can have and needs to be taken into account when analysing the full potential of these technologies. The impact of smart charging and load shifting will be visible in all layers inside the grid. The capabilities of momentarily overloading a power cable by utilising the thermal room inside the load profile will be reduced.

Case studies 1-6 give the impact that the increase of PV power may have on the aggregated load profile which can be seen on a MV cable. When observing the load profiles when PV power is added, the aggregated profile will decrease when low amounts of solar power are added. When enough PV is added the power flow will reverse and power will be delivered to the MV grid. Since the research focuses on heat ($I^2 \cdot R$) the absolute value of the load factor is visualised in Figures 5.7 & 5.8. The overall effect that the addition of PV power has on a normal residential profile is beneficial in terms of overloading capabilities. The overloading factor increases since more valleys inside the profile are created giving the MV cable moments to dissipate some of its stored heat. There is only a slight drop in the overloading factor when 35% of PV is added, this is due to the moment that the highest temperature occurs shifts to a later moment in time, more hours of higher loading are considered when the M-factor is calculated. The impact is not very significant with a gain of around 9% in the most beneficial case study.

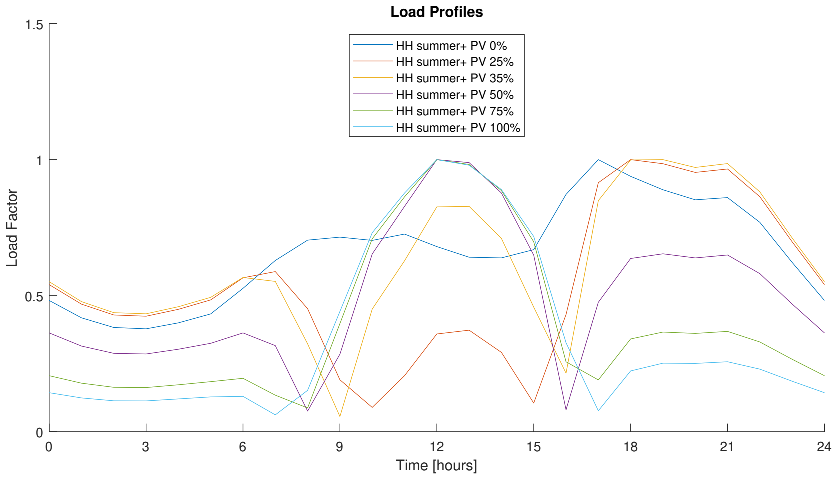

Figure 5.7: Aggregated load profiles for different types of demand or generation

Case Study	1	2	3	4	5	6
HH Summer [%]	100	100	100	100	100	100
PV Summer [%]	0	25	35	50	75	100
M-factor (XLPE)	1.1773	1.2021	1.1631	1.2331	1.2653	1.2656
M-factor (PILC)	1.1527	1.1674	1.1480	1.2007	1.2230	1.2069

Table 5.2: M-factor case studies 1-6

During the winter the peak of the PV power is limited (case study 7-12) and the peak of the profile will not exceed the peak of aggregated household load profile during the winter. This will result in extra dips in the aggregated load profile, which are beneficial for the M-factor which will increase with the addition of PV compared to case study 7. This is beneficial for the DNO since it creates extra ampacity for a MV cable connection. For the summer it is a bit different since the peak of the aggregated load profile with PV added will exceed the peak of the household profile, this has to be incorporated in the calculations of the DNO. The highest temperature in the case studies is happening at the same hour (20h). Since only six hours prior ti the temperature peak and the average of the profile are of importance when calculating the M-factor, the M-factor for these case studies is mainly dependent on the average of the profile, thius result in a maximum increase of around 5%. Both extremes in terms of seasonal variation are examined (winter & summer), in both cases the M-factor increased when more PV power was added to the profile.

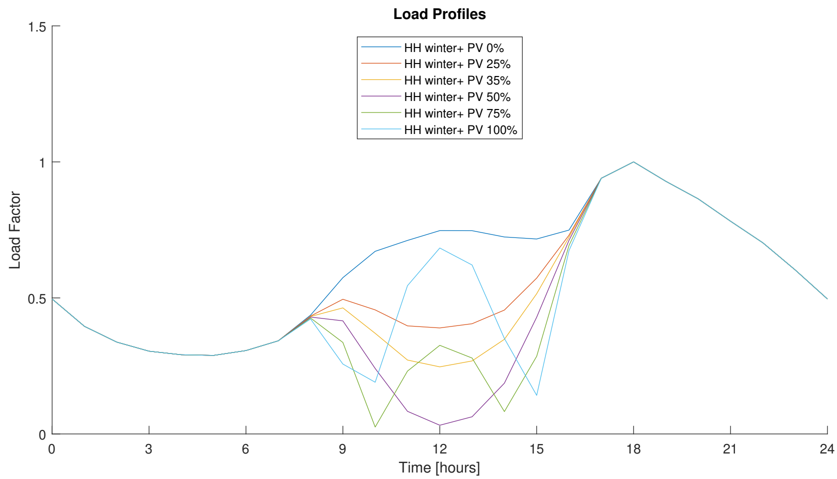

Figure 5.8: Aggregated load profiles for different types of demand or generation

Case Study	7	8	9	10	11	12
HH Winter [%]	100	100	100	100	100	100
PV Winter [%]	0	25	35	50	75	100
M-factor (XLPE)	1.1799	1.2240	1.2365	1.2325	1.2548	1.2367
M-factor (PILC)	1.1520	1.1870	1.1957	1.1665	1.2195	1.2141

Table 5.3: M-factor case studies 7-12

When looking at case studies 13-18 where EV is combined with a household winter profile, the simultaneity which is described in Section 4.1 of these two profiles is highlighted. The simultaneity can also be distracted from Figure 4.1, when people arrive home they plug in their EV and start using their appliances at home. When the amount of EV is increased in the profile the shape of the profile hardly changes. Only the peaks become slightly higher and the valleys slightly lower. This has a slight impact on the M-factor but as these changes in the load profile have a minimal effect on the shape of the profile, the change in the M-factor is also minimal. The maximum change that the case studies show is an increase in M-factor from 1.18 to 1.20. The same applies to PILC cables, the effect is minimal since the shape of the profile is unaltered, and the M-factor increases equally by 2%.

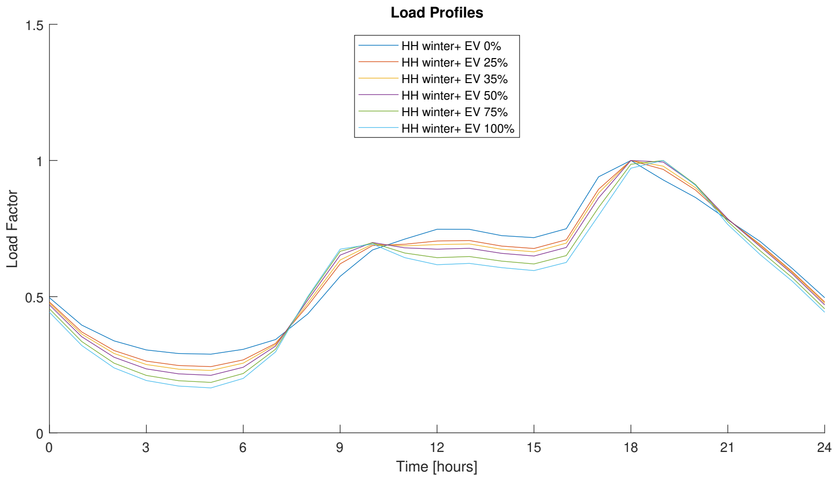

Figure 5.9: Aggregated load profiles for different types of demand or generation

Case Study	13	14	15	16	17	18
HH Winter [%]	100	100	100	100	100	100
EV [%]	0	25	35	50	75	100
M-factor (XLPE)	1.1799	1.1936	1.1931	1.1855	1.1918	1.2014
M-factor (PILC)	1.1520	1.1649	1.1633	1.1547	1.1595	1.1678

Table 5.4: M-factor case studies 13-18

Lastly, case studies 19-24 give the result when the moments of less loading in the aggregated winter household profile are filled with controlled charging of EVs. The aim of these scenarios is to look at the impact that controlling or load shifting has on the overall ampacity of a MV cable connection. The impact that load shifting has on the shape of the load profile is clearly visible in Figure 5.10. Since the ability of the MV cable to dissipate some of its stored heat is diminished, the overloading capabilities will also be reduced. The impact is that the overloading capabilities will drop once the shape of the profile goes towards the shape of continuous loading. This is also observed when looking at the results, in the worst case the M-factor drops to 1.07. This means that the ability to use an M-factor is almost nullified.

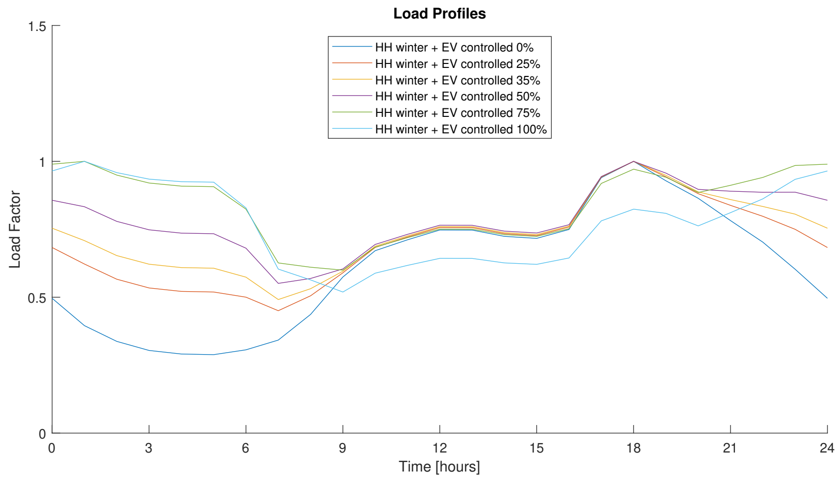

Figure 5.10: Aggregated load profiles for different types of demand or generation

Case Study	19	20	21	22	23	24
HH Winter [%]	100	100	100	100	100	100
EV Controlled [%]	0	25	35	50	75	100
M-factor (XLPE)	1.1799	1.1502	1.1369	1.1162	1.0710	1.1078
M-factor (PILC)	1.1520	1.1279	1.1171	1.1000	1.0605	1.0919

Table 5.5: M-factor case studies 19-24

5.4. SENSITIVITY ANALYSIS PARAMETERS

To evaluate the impact on the uncertainty of parameters which can alter over time or change depending on location, a sensitivity analysis is performed using a range as input during simulation. The load profile will not change during the parameter sweep and the load profile of case study 7 is chosen to be sufficient and relevant during these simulations. The parameters that will be analysed are ground thermal resistance, depth of burial and soil temperature.

5.4.1. CHANGING THERMAL GROUND RESISTANCE

To evaluate how the ground thermal resistance plays a role in determining the ampacity, the ground thermal resistance together with its dependent parameter the thermal diffusivity of soil are changed. If the ground resistivity is lowered the ground diffusivity goes up and vice versa. Firstly the impact on the ampacity of the cable is calculated for continuous loading at nominal ampacity.

In Table A.1 of Appendix A the nominal thermal resistivity of soil in the Netherlands is 1.00 [Km/W], the grid operator deviates slightly from this value in most cases to 0.75 [Km/W]. In some critical cases, the grid operator will do field measurements to validate their view on a certain cable route, but in most cases, a value of 0.75 [Km/W] is taken.

In case the cable is placed in a dry zone the soil thermal resistivity can rise up to 2.5 [Km/W]. The impact of this range of thermal resistivity is calculated and the results are shown in Table 5.6.

Ground Thermal Resistivity [Km/W]	Ampacity [A]	Normalised Ampacity	M-factor	Combined (Ampacity& M-factor)	Normalised
0.50	466	1.23	1.15	1.40	1.19
0.75	**380**	**1.00**	**1.18**	**1.18**	**1.00**
1.00	329	0.87	1.20	1.04	0.88
1.25	294	0.77	1.23	0.95	0.80
1.50	268	0.71	1.23	0.87	0.74
2.00	232	0.61	1.26	0.77	0.65
2.50	208	0.55	1.29	0.71	0.60

Table 5.6: Ampacity for a changing ground thermal resistance (XLPE 3x1x240mm2)

Since the thermal ground resistance has a great influence on the ampacity of a cable connection this parameter must be measured accurately. The spot with the highest ground thermal resistivity can reduce the ampacity of a whole cable connection. It will not only affect the ampacity of a connection as seen in Figure 5.1, where the ampacity is calculated for different soil thermal sensitivities, but also the time constant of the thermal process changes. This will result in a different M-factor since the M-factor is dependent on the time constant of the total thermal response of the system.

The soil thermal resistivity is changed in steps over a range of 0.5 to 2.5 [Km/W] with a burying depth of 1000 [mm] and an ambient temperature of 15 [°C]. The continuous ampacity for a nominally loaded cable is given in the second column with the reference at 0.75 [Km/W]. This is normalised on the reference in the third column. The ampacity increases and decreases very rapidly over the trajectory of the thermal resistivity range. When the soil thermal resistance is more favourable than 0.75 [Km/W] for instance 0.5 [Km/W] the ampacity for a nominally loaded cable can increase by 23% but when the soil thermal resistivity is less favourable up to 2.5 [Km/W] it can reduce its nominal ampacity with 45%.

When the soil thermal resistivity is increased so is the time constant of the whole thermal system. The heat is transferred a lot slower and this has an influence on the M-factor. This effect can be observed in the fourth column of the table, where the M-factor for the load profile of case study 7 is used. When the ampacity and the M-factor are combined the true ampacity for this specific load profile can be obtained. When the soil thermal resistivity is decreased the ampacity increases by about 20% per 0.25[Km/W] and when the soil thermal resistivity is increased the combined ampacity drops with an average of 8% per 0.25 [Km/W].

Thus to increase the accuracy of calculating the ampacity of MV cables extra field measurements are needed close to MV connections to have a realistic view of the current carrying capacity of cable connections. The impact of a slight error is significant as seen above in Table 5.6, these measurements can greatly influence the way the DNO utilizes its MV cables since this can have an impact on the lifetime of the cable.

5.4.2. CHANGING BURYING DEPTH

The burying depth can vary over the trajectory of the cable, so it is important to know what the influence will be on the ampacity. To analyse this result the ground thermal resistance will be unchanged and the depth of burial will be altered in steps to see the impact on the continuous loading of a cable and the impact when a load profile is applied. When the depth of installation is altered also the thermal dynamics of the system change, this has a slight influence on the M-factor. All the values are compared to the standard burying depth of 1000 [mm] beneath the surface.

Depth of Burrying [mm]	Ampacity [A]	Normalised Ampacity	M-factor	Combined (Ampacity& M-factor)	Normalised
500	419	1.10	1.15	1.27	1.07
750	395	1.04	1.17	1.21	1.03
1000	**380**	**1.00**	**1.18**	**1.18**	**1.00**
1250	370	0.97	1.19	1.16	0.98
1500	362	0.95	1.20	1.14	0.97
1750	355	0.94	1.20	1.13	0.95
2000	350	0.92	1.21	1.11	0.94
2500	342	0.90	1.22	1.09	0.93
5000	320	0.84	1.24	1.04	0.88

Table 5.7: Ampacity for a changing depth of burial of MV cables (XLPE 3x1x240mm2)

Table 5.7 shows how the ampacity of continuous loading in the second column. If the load profile of case study 7 is applied a M-factor for the profile is calculated. As stated at the beginning of this section the M-factor will change while applying the same load profile due to the changing thermal dynamics of the system. This can be seen in the column "M-factor" of the table.

When the burying depth is increased the ampacity is decreased, for the M-factor this is the other way around because the time constant of the system increases and more thermal room is created in the profile to momentary overload the cable since there are also moments of less loading in the load profile. When these two are combined the impact of a changing burying depth can be analysed.

As a result, placing the cable shallower in the ground can have a slightly positive effect on the overall cable ampacity. For every 25mm that the cable is placed deeper the ampacity for a load profile that is similar to case study 7 the ampacity decreases by 1.5%.

For every 25mm that the cable is placed shallower compared to 1000 [mm] the ampacity for the same load profile increases by about 3.5%. This can also reduce costs since less ground has to be dug out to make room for a cable trench. Two important notes to take into account are that by placing the cable less deep, the chance of defects due to digging damage of contractors which can happen during the lifetime of the cable might increase, and the DNO has set a burying depth for MV cables at 800 [mm] [32]. Since the gain in ampacity is very limited, the DNO has to weigh these factors before coming to a final conclusion on altering the burying depth of MV cables.

5.4.3. CHANGING SOIL TEMPERATURE

A lot of infrastructures are present below the surface, some of which carry heat or produce heat. This heat just like the heat generated by a power cable travels outwards and increases the temperature of the ambient. Not only heat from other man-made heat sources affect the temperature of the surrounding of a buried power cable, but also the heat that is radiated from the sun which heats up the surface travels through the ground with a certain temperature gradient downwards from the surface which is dependent on the type of material and temperature difference. This process is rather slow but the seasonal weather conditions can be observed when comparing the soil temperature at different times during the year.

Different simulations are done in steps of 5 [°C], using a burying depth of 1000 [mm] with a ground thermal resistance of 0.75 [Km/W]. When the temperature of the ambient is lower the difference in temperature between maximum sheath temperature when ground dehydration should be avoided is higher. When the difference is higher the cable can dissipate more heat to its surrounding, this will increase ampacity.

Soil Temperature [C]	Ampacity [A]	Normalised Ampacity	M-factor	Combined (Ampacity& M-factor)	Normalised
0	466	1.23	1.18	1.45	1.23
5	439	1.16	1.18	1.36	1.16
10	411	1.08	1.18	1.28	1.08
15	**380**	**1.00**	**1.18**	**1.18**	**1.00**
20	347	0.91	1.18	1.08	0.91
25	310	0.82	1.18	0.96	0.82
30	268	0.71	1.18	0.83	0.71

Table 5.8: Ampacity for a changing soil temperature (XLPE 3x1x240mm2)

In Table A.1 of Appendix A the thermal characteristics of the soil in the Netherlands are given. It states an average soil temperature of 15 [°C] which can decrease during the winter to 5 [°C] and rise in the summer to 20 [°C]. In Section 2.3 a simplified formula (2.25) of field measurements in the port of Antwerpen is given, this formula is based on field measurements. It gives insight into the seasonal variation of the ground temperature, which in this case varies between 8 and 26 [°C]. The impact of this is calculated and the results are given in Table 5.8.

Comparing the results in a similar way as done for the depth of burial using the load profile of case study 7, the results are compared to the average stated in the site reference. When the nominal ampacity is observed in the second column the ampacity is highly dependent on soil temperature. For every 5 [°C] that the temperature increases the ampacity decreases by about 10% and when the soil temperature decrease ampacity increases by about 8%. Soil temperature will be lower during the winter and energy demand will be higher during this time of the year. The lower soil temperature can be used as an advantage to allow higher loading during the winter. Again taking the average temperature of 15 [°C] as the reference the nominal current is normalised to this value in the third column of Table 5.8. With a constant M-factor for all the different soil temperatures a combined factor can be calculated. Since the M-factor is equal for all the cases the end result doesn't differ from the results stated above.

5.4.4. SIMPLIFICATION OF CABLE MODEL

To analyse what error is introduced if certain components of the cable model are removed, the model is reduced. The constructed analytical transient thermal model is taken as a base case.

When three single-core XLPE cables are placed in trefoil compared to flat formation the magnetic fields are kept to a minimum, this will reduce the current and heating in the sheath. Another advantage of trefoil formation is that it saves space, a disadvantage of placing cables in trefoil formation is that they are placed very close to each other reducing the capability to easily dissipate heat. The heat produced by each single core cable will influence each other more in trefoil than flat formation.

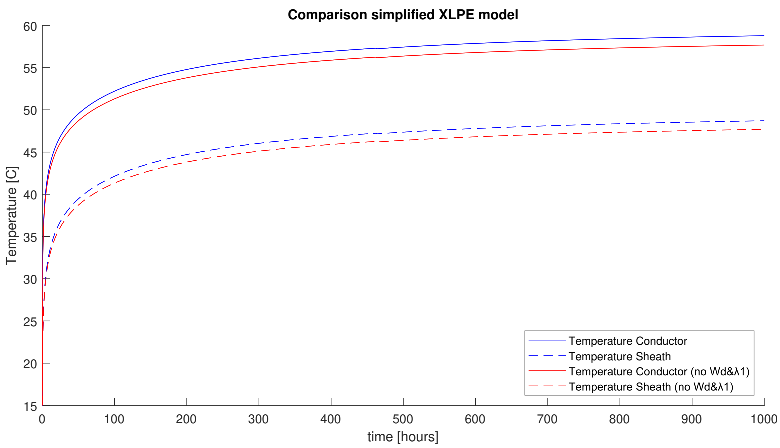

Figure 5.11: Removed dielectric loss and sheath loss

The sheath loss and dielectric loss are very limited in a MV cable placed in trefoil, so in order to see what their impact is on the ampacity they are removed from the model. Together they account for roughly 3% of the total loss. The results are given in Figure 5.11, since losses are removed the temperature will decrease. The temperature decrease is very minimal, about 1 [°C] and the M-factor is not affected by this change. The error in sheath temperature will therefore be 3% on the temperature increase from the initial temperature.

As shown, the contribution of the dielectric loss in medium voltage cable systems is very limited on the total temperature rise of the cable under loading. The dielectric loss when 10 [kV] is applied on the XLPE cable only accounts for roughly 0.2% of the total loss when a nominal load of 380 [A] is applied. For this reason, the influence of voltage variation due to decentralized in-feed or loading can and will be neglected.

5.4.5. MONTE CARLO ANALYSIS OF CONDITION UNCERTAINTY

The created deterministic model calculates the ampacity and the M-factor using different ambient conditions and parameters. In the previous sections, the individual impact of altering the ambient conditions is examined. Since the conditions have an impact on the ampacity and these conditions of the ambient of a MV cable can change over the trajectory of a connection or in some cases are unknown. A Monte Carlo simulation is performed on the uncertainty of these conditions. By using a fixed load profile, but defining a range for the ambient conditions, the impact of the uncertainty can be simulated. The connection between these parameters is unknown and is taken to be uncorrelated. It is taken that the distribution of these parameters is uniform, due to a lack of measurements and data. The range of the parameters is taken from the site reference conditions in the Netherlands from Appendix A and the from Section 2.3:

- Burying depth 0.8 - 1.2 [m]
- Ambient temperature 5 - 20 [°C]
- Ground thermal resistivity 0.75 - 2.0 [Km/W]
- Number of simulations 10,000

When using the aggregated load profile of winter household demand (Case Study 7) and the range of conditions specified above the ampacity and the M-factor can be calculated for different conditions. The ampacity is compared with the nominal ampacity for constant loading with ground conditions of 1000 [mm], 15 [°C] and 0.75 [Km/W], which yield an ampacity of 380 [A] when drying out of soil should be avoided. The resulting maximum ampacity for each simulation is divided by the nominal ampacity of 380 [A] to normalize since this ampacity is used for simulations and grid analysis. If the ampacity times the M-factor is lower than one the cable will violate its thermal limits. The yellow line shows the limit where the ampacity times the M-factor is one. If the DNO wants to avoid soil dehydration a sheath temperature of 45 [°C] is leading. Thus all the simulation

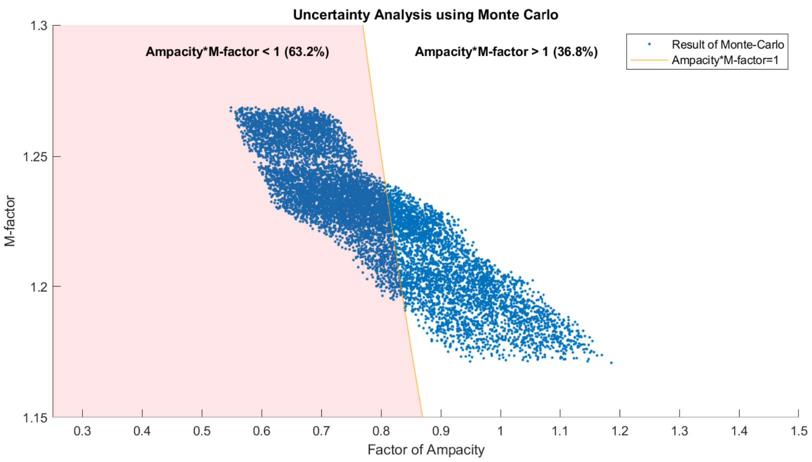

Figure 5.12: Ampacity & M-factor for different ambient conditions (Profile Case Study 7)

results should be on the right side of the yellow line.

In Figure 5.12 the results of the Monte Carlo analysis for varying conditions with case study 7 are visualised. Only 37% of the simulations stay within the thermal limits of the modelled XLPE cable. This shows that when this load profile occurs and hardly any information is present about the ambient conditions only one-third of the time the cable does not exceed its limits.

The same analysis could be done for case study 23, where load shifting is incorporated. In the previous analysis, it could be seen that the M-factor for this case study was significantly lower, 1.07 compared to 1.18. The same set of conditions is taken and ten thousand simulations are performed. Figure 5.13 shows the result. Yet again it clearly shows that a lot of simulations yield an undesirable outcome. In this analysis only about 16% of the simulations are within the limit. The percentage dropped when being compared to case study 7, due to the extra load in the system at moments of less loading. This has to be taken into consideration when fully utilising the available ampacity of a load profile of a cable connection in time.

This shows the impact that uncertainty of conditions can have on the ampacity of a cable connection. The only way to mitigate this uncertainty is to take field samples along the trajectory of the cable connection to determine the ground thermal resistivity, placement depth and to add sensors to analyse the ambient temperature in the ground surrounding the cable. When this data is gathered and used in the model, a more accurate prediction could be done on the maximum ampacity. If the gathered data varies a lot the worst-case calculation for the combination of ampacity and M-factor should be taken to define the ampacity of the whole connection. If no further research is done for ground parameters and the range that is specified is occurring in the Netherlands.

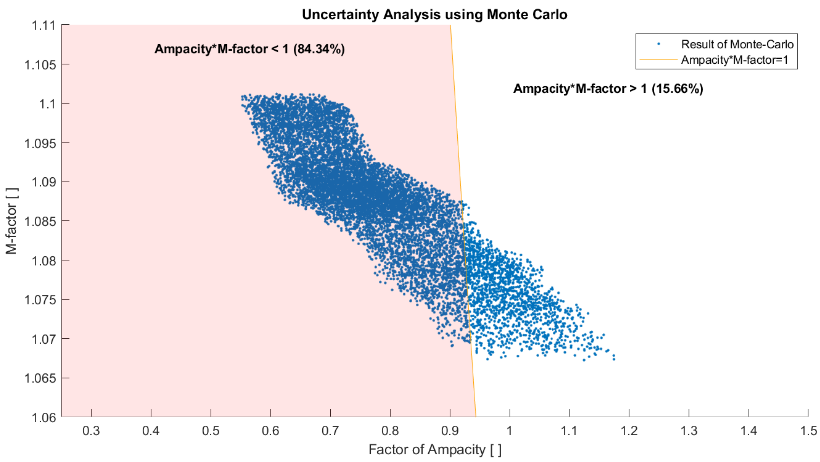

Figure 5.13: Ampacity & M-factor for different ambient conditions (Profile Case Study 23)

In both cases more than 50% (63.2% and 84.34%) of the cases, the ground temperature will exceed the threshold for ground dehydration. Inside a circle that will circumscribe the conductors the ground will be dehydrated, resulting in a bigger surface area to dissipate the generated heat. This slightly increases the ampacity of the cable connection. If the slightly higher ampacity for certain site conditions is still violated then the dehydrated circle circumscribing the conductors will increase in diameter and this will have a drastic negative effect on the ampacity of the cable connection.

5.5. THEORETICAL EXAMPLE

The MV grid is redundant to reestablish the power flow in a small period of time through another connection. This redundancy is established by the DNO through two types of grid structures:

- **Ring**, loads are connected in a ring-type topology with an opening at a certain point (operated radially) to prevent circulating currents and make fault localisation possible.
- **Meshed**, this topology consists of multiple rings (operated radially) with interconnection(s) between them to take over some of the load during maintenance or faults.

Although both topologies are used in MV distribution grids, the MV network is operated radially. Redundancy is established by shifting the opening in the ring to any switchgear location inside the ring during maintenance or faults, to guarantee a quick restoration of the power flow. After the fault or maintenance has been cleared the grid topology is restored to its original formation.

In order to cope with the extra load during the shift of the opening in the ring, both branches in the ring are nominally loaded not more than 60%. If a worst-case fault occurs in the first section of the opposing half of the ring. The supply is restored by closing the ring opening and the loading on the first cable section in the healthy half of the ring is increased to 120%, under the restriction that within 7 days the normal grid topology must be restored. The event is simulated at day 25 which will be cleared after 7 days at day 32.

As shown in Section 5.3 for a conventional aggregated daily household demand load profile, the M-factor is approximately 1.18. In this case, the 20% overload is no problem and the temperatures will stay within limits. This is due to the low loading before the fault occurred, the overloading being almost equal to the M-factor and the slowness of the temperature accumulation in the MV cable.

For case studies 7 and 23, the M-factor deviates a lot due to the differently shaped load profile. In case study 7 for a normal aggregated winter residential load profile the M-factor is 1.18 and for use case 23 where controlled EV charge is added the M-factor drops to around 1.07 (see Section 5.3). In this case, the overloading at 120% is not close to the permitted overloading factor of the load profile of 107%. Simulations are done in COMSOL to get a better insight into the temperature progression during maintenance and faults. An ideal distribution of loading both ends in the MV ring with an aggregated load profile with its peak at 60% of its nominal ampacity is taken as normal operation. As stated earlier the first cable section of the ring is in the case of minimal DER the section where the highest loading will take place. The results of this section are taken and the assumption is made that a minimal amount of DER is present in the MV ring and almost all the energy is supplied by the MV transport/distribution station. The thermal response of case study 23 is visualised using a ρ_T of 0.75 and 2.0 [Km/W] in Figure 5.14 & 5.15 respectively. The overloading capabilities (M-factor) are not being used, to see in the current situation how the uncertainty of ground thermal resistivity affects cable temperatures during maintenance and faults.

With a low thermal resistivity of $\rho_T = 0.75$ [Km/W] the temperatures of the conductor and sheath stay well below the thermal limits, see Figure 5.14. Since ground dehydration only occurs after longer periods of time that the temperature of 45 [°C] is being violated, the main goal is for the conductor temperature to stay below 90 [°C]. For the full period of 7 days, the temperature of the conductor is not exceeding 90 [°C].

If the same load profile is used but the thermal resistivity of the ambient is increased from 0.75 to 2.0 [Km/W], the impact (Figure 5.15) that uncertainty has on faults and maintenance is highlighted. Within two days after the event, the temperature of the conductor exceeds the limit of 90°C. This can lead to a meltdown of the dielectric resulting in a breakdown of the MV cable. Since the DNO is already in a situation where it is using its N-1 the breakdown of an extra section can have a big impact. This simulation shows the urge for the DNO to start mapping the thermal resistivity in their operating area. This will play a vital role in the ability to fully utilize the ampacity but not shorten the lifetime of all MV cable connections.

5

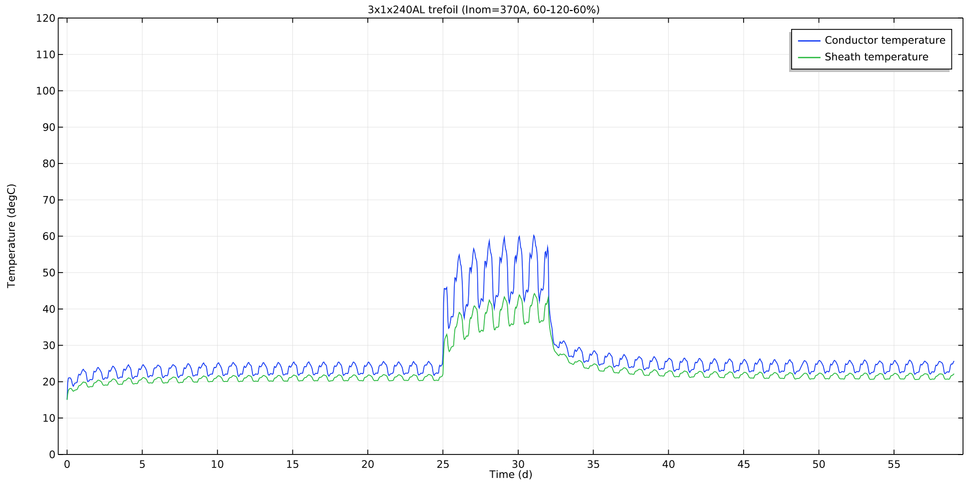

Figure 5.14: Temperature response during maintenance or faults (Profile Case Study 23, ρ_T=0.75[Km/W])

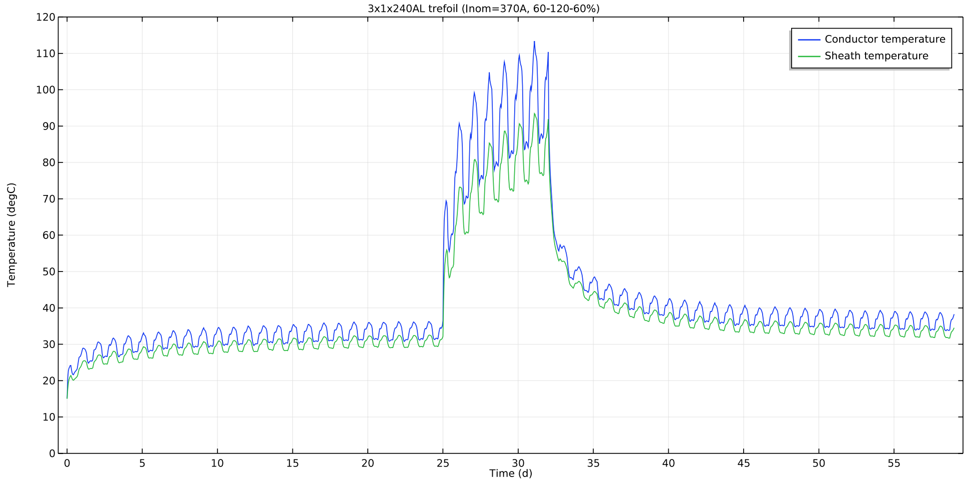

Figure 5.15: Temperature response during maintenance or faults (Profile Case Study 23, ρ_T=2.0[Km/W])

6
Conclusion & Recommendations

The potential gain of utilizing the thermal room inside a load profile during ampacity modelling is summarized, together with how the overloading capabilities change for different case studies. How uncertainty of site conditions influence the accuracy of modelling. Which parameters have the most influence when modelling the ampacity of an underground MV cable connection and the differences in the analytical and FEM model are emphasised to make a consideration of which model to use when modelling the ampacity and overloading of MV cable connections.

To conclude the research, the research questions are answered and relevant points for future research are given.

6.1. Impact

The methods described in this research could be used by the DNO to make a considered decision about the ampacity for MV cables during normal operation, faults and maintenance. When the right set of parameters is known this method could give more insight than just applying the ampacity tables in the IEEE-standard 834-1994 [33] or the ampacity stated in the brochure of the cable manufacturer (e.g. [22]). It also shows the possibility of utilising the MV cable network ampacity in a more optimal way. By considering the shape of the cyclic load profile, the peak of the load profile may exceed the nominal continuous ampacity and preserve and not violate thermal limits.

The impact that a changing reoccurring load profile might have on the current methodology of a DNO, is truly dependent on the development of the shape of the load profile. The overloading capabilities of MV cables are dependent on the site conditions and the load profile which it has to transport on a reoccurring daily basis. The range over which a DNO has the ability to overload a MV cable due to thermal room in the aggregated load profile is significant. The results from the case studies show that overloading in the range of 1.07-1.27% is possible. It is hard to pinpoint one specific overloading factor that could be applied to all the MV cable connections. The overloading capabilities are hardly affected by the extra demand from normal uncontrolled EV charge since the simultaneity of the profile is very high with the aggregated household demand profile, and the change in load profile is very limited. If the charge of EV will be controlled and the demand is shifted to moments of less congestion the peak power will be limited reducing peak load but the shape of the load profile changes drastically. This change will limit the overloading capabilities of a MV cable since the moments of lower loading are becoming less deep and long preventing the cable to cool down.

The direct impact that parameter uncertainty has on the normal daily operation of MV cables is very limited. As stated in Section 5.5, MV cables are loaded at about 60% to ensure redundancy (N-1) in the grid. This is done to facilitate quick restoration of power during faults or maintenance. This lower loading of the MV cable compared to the nominal current is beneficial when no ambient parameters are known. A problem could occur when the loading is increased and the ambient parameters are unknown, simulations have shown that with unfavourable site conditions this can already occur after two days. The time of extra loading due to faults or maintenance is limited and the time it takes to dehydrate soil is rather large, the DNO only has to consider the conductor temperature not exceeding 90 [°C]. Whether the conductor temperature exceeds the limits is very dependent on the thermal resistivity and ambient temperature of the ground. The overloading capabilities of a load profile are also beneficial during these events if they are not already being utilized.

6.2. ANSWERS TO RESEARCH QUESTIONS

- *What is the impact of different load profiles (case studies) due to changing loads and distributed generation (e.g. PV & EV) on the ampacity of MV cables in the grid?*

  The impact is that the overloading factor will increase or decrease with the addition of DER or EV. When the M-factor increases this has a beneficial effect on the overall ampacity of the MV cable. If load shifting will take place and the load profile will tend to flatten during the course of 24 hours the overloading abilities will disappear. The impact of the reduced overloading capabilities should be considered when the benefits of load shifting in the LV are presented. The potential gain above nominal ampacity is shown using the different case studies, the maximum overloading factor for a certain case study was as high as 26% and the minimum was 7%. If a general load pattern for residential MV rings can be obtained the nominal ampacity rating of underground MV cable connections can be higher than the current nominal ampacity. This shows the potential benefits that this method can have to (temporally) solve contingencies and postpone investments.

- *Which variables of the model have the most impact on the ampacity and overloading capabilities of MV cables?*

  The parameter which has the most influence on the ampacity of the whole cable connection is the thermal resistivity of the material surrounding the cable. If this parameter deviates over a bandwidth of 0.75-2.0 [Km/W] it will result in a maximum reduction of the current nominal ampacity of 39%. Due to the lower loading of MV cables as shown in Section 5.5, most of the thermal limits are not being violated at the moment during normal operation. The effect that the changing burying depth has on the ampacity is almost negligible. If the MV cable is placed 250 [mm] deeper or shallower than 1000 [mm] compared to the surface will result in an ampacity loss of 3% or gain of 4% respectively. Lastly, the ambient temperature of the MV cable will have a more severe impact than the burying depth. The change in ambient temperature will result on average in a 9% decrease of ampacity for every 5 [°C] that the temperature rises compared to 15 °C and an increase in ampacity of around 8% for every 5 [°C] that the temperature drops.

- *Which assumptions can be taken to simplify the method and still have a representative outcome?*

Both the dielectric and sheath loss can be neglected when modelling a single-core XLPE cable in trefoil at 10kV. The total loss of both factors combined is roughly 3% of the total loss, and the error in temperature is roughly 1 [°C]. The impact of a varying dielectric loss which can be present due to voltage variations which are caused by DER will also be negligible.

The DNO has to make the consideration to accept this error if this simplification can save a lot of computational or time to construct the model. Considering that a DNO has a lot of kilometres of cable, if they want to model all of them, these losses might be neglected.

6

- *Which field measurements need to be taken to increase accuracy and aid with validation of modelling the ampacity of MV cable connections?*

The uncertainty due to the absence of accurate measurements is rather high. A large bandwidth is taken for a set of ambient parameters based on site reference conditions (Appendix A), to simulate different ground conditions which can be expected. The results show a deviation from the standard ampacity which the DNO uses in their network when site conditions are unknown.

The placement depth of a MV cable can not be altered since the cable must be installed on the correct depth determined in the policy of the DNO. If it would be altered only a minor increase in ampacity will be achieved, of around 3% per 250 [mm]. More insight can be gained by measuring the ambient temperature and thermal resistivity of the soil. The results show a maximum reduction of 45% of the nominal ampacity if the ground thermal resistivity is significantly higher, a dry zone, ($\rho_T = 2.5[Km/w]$) than the assumed ground thermal resistance of $\rho_T = 0.75[Km/W]$. If this reduction in the ampacity is not incorporated into the network the lifetime and reliability of the MV cable will be reduced. The ambient temperature of a cable connection is relatively easy to measure and together with a temperature measurement of the outside of the cable can narrow down the nominal ampacity and prevent dehydration of the soil. To determine the ampacity of a MV cable connection properly at least the temperature and ground thermal resistivity need to be measured.

Adding extra measurements will greatly improve the accuracy of modelling and provide insight into thermal violations. This can have great benefits in the long run since violating the thermal limits will influence the remaining lifetime of the cable connection. The uncertainty simulation using a normal residential load profile (case study 7) showed that when the ampacity is based on a fixed value but in reality, the ambient conditions differ, the thermal limits of around 63% of the connection if they were being fully utilized ampacity wise will exceed their thermal limit of 45 [°C] sheath temperature. Every underground MV connection is unique, to gain full insight a lot of measurements need to be taken by the DNO, also in order to see how much the ground thermal resistivity and temperature change in a certain area.

6.3. Recommendations

Recommendations towards the DNO based on this study are:

- Gain extra knowledge on the ground conditions (especially ground thermal resistivity) throughout the whole area of operation. With the aid of measurements and additional studies narrow down the bandwidth of the uncertainty of ambient conditions. This can significantly improve the accuracy when determining the ampacity of MV cable connections.
- The DNO can start utilizing the thermal room inside a known reoccurring load profile.
- Good caution must be taken when implementing the M-factor. When the shape of the load profile changes significantly a new M-factor should be obtained.
- Add temperature sensors next to critical MV cable connections to monitor the sheath temperature during normal operation, to prevent dehydration of the soil surrounding the cable. With this temperature, the constructed models can be validated and the conductor temperature can be derived if the current is known.
- When calculating the nominal ampacity of a MV cable connection, the thermal resistivity and other site conditions must be taken into account. By doing so the temperature of the conductor and the outside of the cable will stay within their limit, significantly increasing the lifetime and reliability of the MV cable network.

6.4. Future work

Extra study is recommended on the next topics to gain more insight into this topic:

- Cables in ducts and pipes must be evaluated, which is very case specific but will also influence the thermal response, impacting the ampacity and the overloading capabilities of a MV cable connection.

- Implement weather information to simulate how the temperature of the soil changes over the course of a simulation.
- Validate the analytical model of a XLPE cable by real-time current and temperature measurements in the field.
- Study how soil dehydration (drying-out) occurs and under which circumstances and see what the impact of groundwater levels is on soil thermal resistivity and rehydration of the soil.
- Add the effect that other heat sources e.g. parallel or crossing cables and heat pipes have on an underground MV cable connection.
- Define industrial or mixed load profiles and apply the same methodology to see the impact that the shape of these profiles have on the overloading capabilities of MV cable connections.

A

SITE REFERENCE CONDITIONS NL

Thermal characteristics of the soil		
Thermal resistivity, nominal	1,00	K·m/W
It is recommended that a survey of the thermal characteristics of the soil is carried out for critical cable links.		
Thermal resistivity, dry zone	2,5	K·m/W
It is recommended that a survey of the thermal characteristics of the soil is carried out for critical cable links.		
Temperature, maximum	20	°C
Temperature, winter	5	°C
Temperature, average	15	°C
Depth of laying of cables		
Up to 30 kV	0,7 to 1,0	m
Above 30 kV	1,2	m
Air ambient temperature		
Maximum	30	°C
Minimum	-10	°C
Average	20	°C
Cyclic ratings		
Critical temperature	30	°C
The critical temperature is highly dependent on soil composition and location. It may also vary due to seasonal influences and/or cyclic loading. It is recommended to investigate the critical temperature during a soil survey, unless it can be demonstrated that no drying out of the soil will occur.		
Solar radiation		
Intensity of solar radiation	1 000	W/m^2

The two zone model is regularly used to calculate the current rating of MV cable systems and incidentally for HV systems. The parameter used to define the boundary between wet and dry zones is the absolute temperature, isotherm at this boundary, usually in the range between 30 °C (MV cables) and 50 °C (HV cables).

Cable circuits are taken to be thermally independent if the separation is not less than 3 m. For cables installed deeper than 3 m, such as in horizontal directional drilling, the minimum separation is not less than 5 m to consider a cable circuit as thermally independent.

Figure A.1: Site reference conditions NL [18]

B

Calculation of $\frac{\theta_R(i)}{\theta_R(\infty)}$

The calculation from the IEC60853-2-1 [17] used to obtain $\frac{\theta_R(i)}{\theta_R(\infty)}$ is given below. It can be used for the two-looped thermal equivalent network. For both the conductor and sheath respectively the attainment factors ($a_1 \& b_1$) are calculated. They give a factor of how the temperatures respond to an applied nominal continuous load over time towards from $t = 0$ to ∞.

$$a_1(t) = \frac{T_a(1-e^{-at}) + T_b(1-e^{-bt})}{T_A + T_B} \quad \Rightarrow \quad \theta_c(t) = a_1(t)\theta_c(\infty) \tag{B.1}$$

$$b_1(t) = \frac{-Ei(-\frac{D_e^2}{16t\delta}) - (-Ei(-\frac{L^2}{t\delta}))}{2\ln\frac{4L}{D_e}} \quad \Rightarrow \quad \theta_e(t) = b_1(t)\theta_e(\infty) \tag{B.2}$$

Factor k gives the ratio of the cable outside surface temperature rise above ambient to conductor temperature rise above ambient under steady conditions. This is needed since the temperature of the outside of the cable will not reach the same temperature as the conductor.

$$k = \frac{\theta_e(\infty)}{\theta_R(\infty)} = \frac{W_l T_4}{W_c(T_A + T_B) + W_l T_4} \tag{B.3}$$

Combining all the factors the required ratio can be obtained to calculate the temperature response of the conductor.

$$\frac{\theta_R(i)}{\theta_R(\infty)} = a_1(i)\ (1 - k\ +\ kb_1(i)) \quad \text{with } i = 3600t \tag{B.4}$$

C

Material Properties & Dimensions used for Modelling

The dimensions of the used TKF single core 240mm^2 12/20kV CU XLPE cable which is placed in trefoil in both models are given together with the material properties of the layers inside the cable and the ambient material. The cable is modelled in perfect trefoil formation where the outsides of the cables are touching. Table C.1 gives the cross-section area in mm^2 is given together with the diameter over each layer. Table C.2 describes each material in three properties which are needed to model the thermal response, namely the density, the thermal conductivity and the heat capacity at constant pressure of the material. Additional information used during simulations is given underneath:

- XLPE $\tan(\delta) = 0.004$
- $\rho_T = 3.5$ [Km/W]
- average $L = 1$ [m]
- average $\theta_a = 15$ [°C]
- Diffusivity of soil (@ $\rho_T = 0.75$ [Km/W]) $= 0.6 \cdot 10^{-6}$ [m^2/s]
- Volumetric specific heat of XLPE & PE $= 2.4 \cdot 10^6$ [J/(m^{3}K)]
- Conductor $R_{ac}(@\ 90°C) = 0.162 \cdot 10^3 [\Omega/\text{m}]$ (Analytical model)
- Conductor $R_{ac}(@\ 55°C) = 0.143 \cdot 10^3 [\Omega/\text{m}]$ (Analytical model)
- Conductor $R_{ac} = 0.1246 \cdot 10^3 (1 + 0.00429(\theta_c - 20)) [\Omega/\text{m}]$ (FEM)

- Sheath $R_{ac} = 0.638 \cdot 10^3\,[\Omega/\mathrm{m}]$
- $U_0 = 10$ [kV]
- $\omega = 2\pi f\,[\mathrm{rad/s}]$

Conductor area [mm^2]	Sheath area [mm^2]	Conductor [mm]	Dielectric [mm]	Sheath [mm]	Cable [mm]	Capacitance [μ F/km]
1x240	25	18.6	31.9	36.8	44	0.31

Table C.1: Dimensions TKF single core 240mm^2 CU 12/20kV [22]

	Density [kg/m^3]	Thermal conductivity [W/(mK)]	Heat capacity at constant pressure [J/(kgK)]
Soil	1400	1/0.75	800
Aluminium	2700	237	904
Copper	8960	401	384
Polyethylene (& XLPE)	930	0.2857	1900

Table C.2: Material properties FEM

Bibliography

[1] Ministerie van Economische Zaken en Klimaat. *Klimaatakkoord*. May 2021. URL: https://www.rijksoverheid.nl/onderwerpen/klimaatverandering/klimaatakkoord.

[2] D. Hammer N. Refa and J. van Rookhuijzen. *Elektrisch rijden in stroomversnelling - Elektrificatie van personenauto's tot en met 2050*. Q3 2021. URL: https://elaad.nl/wp-content/uploads/2022/05/2021Q3_Elaad_Outlook_Personenautos_2050.pdf.

[3] PWC. *De energietransitie en de financiële impact voor netbeheerders – in opdracht van Netbeheer Nederland*. Apr. 2021. URL: https://www.netbeheernederland.nl/_upload/Files/PwC_De_energietransitie_en_de_financiele_impact_voor_netbeheerders_15_04_2021_193.pdf.

[4] D.M. Simmons. *Calculation of the Electrical Problems of Underground Cables*. General Cable Corporation, 1932.

[5] J. H. Neher and M. H. McGrath. "The calculation of the temperature rise and load capability of cable systems". In: *Transactions of the American Institute of Electrical Engineers. Part III: Power Apparatus and Systems* 76.3 (1957), pp. 752–764. DOI: 10.1109/AIEEPAS.1957.4499653.

[6] Bernard Jr, Gary Orlove, and Donna Peters. "The relationship between current load and temperature for quasi-steady state and transient conditions". In: *Proceedings of SPIE - The International Society for Optical Engineering* (Mar. 2000). DOI: 10.1117/12.381580.

[7] F. Wild et al. "Dynamic Rating Systems in General and in a Hibrid 150 KV Transmission System". In: *Jicable '07* (2007), pp. 1–5.

[8] F. de Leon. "Major factors affecting cable ampacity". In: *2006 IEEE Power Engineering Society General Meeting*. 2006, 6 pp.-. DOI: 10.1109/PES.2006.1708875.

[9] Faruk Aras and Yunus Biçen. "Thermal modelling and analysis of high-voltage insulated power cables under transient loads". In: *Computer Applications in Engineering Education* 21 (Sept. 2013). DOI: 10.1002/cae.20497.

[10] G. J. Anders. *Rating of Electric Power Cables*. New York, USA: Mc-Graw-Hill, 1997.

[11] "Current rating equations (100 % load factor) and calculation of losses – General". In: *Electric cables – Calculation of the current rating*. Vol. IEC60287. 1-1. 2014-11, pp.1–142.

[12] F. H. Buller. "Thermal transients on buried cables". In: *Electrical Engineering* 70.7 (1951), pp. 603–603. DOI: 10.1109/EE.1951.6436706.

[13] F. C. Van Wormer. “An Improved Approximate Technique for Calculating Cable Temperature Transients [includes discussion]”. In: *Transactions of the American Institute of Electrical Engineers. Part III: Power Apparatus and Systems* 74.3 (1955), pp. 277–281. DOI: 10.1109/AIEEPAS.1955.4499079.

[14] J van de Vyver, T Vandoorn, and P Lauwers. “Measurement, Modelling and Real-time calculation of Medium Voltage Cable Temperatures”. In: *CIRED 25th International Conference on Electricity Distribution* (June 2019), n 775.

[15] Marc Diaz-Aguiló and Francisco de León. “Introducing Mutual Heating Effects in the Ladder-Type Soil Model for the Dynamic Thermal Rating of Underground Cables”. In: *IEEE Transactions on Power Delivery* 30.4 (2015), pp. 1958–1964. DOI: 10.1109/TPWRD.2015.2390072.

[16] Stedin. *Internal Document*.

[17] *NEN-IEC 60853-2-1:2007(EN) Electric cables - Calculation of the cyclic and emergency current rating of cables - Part 2: cyclic rating of cables greater than 18/30 (36) kV and emergency ratings for cables of all voltages*. Standard. Geneva, CH: International Electrotechnical Commission, Oct. 2007.

[18] *NEN-IEC 60853-3-1:2017(EN) Electric cables - Calculation of the current rating - Part 3-1: Operating conditions - Site reference conditions*. Standard. Geneva, CH: International Electrotechnical Commission, June 2017.

[19] Carson Bates, Keith Malmedal, and David Cain. “Cable Ampacity Calculations: A Comparison of Methods”. In: *2015 IEEE Rural Electric Power Conference*. 2015, pp. 81–87. DOI: 10.1109/REPC.2015.13.

[20] Osama Gouda et al. “Experimental study for drying-out of soil around underground power cables”. In: vol. 9. Sept. 1992, 99–102 vol.1. DOI: 10.1109/MWSCAS.1992.271324.

[21] Jianmei Jiang et al. “Experimental study of the effect of shallow groundwater table on soil thermal properties”. In: *Frontiers of Earth Science* 10 (June 2015). DOI: 10.1007/s11707-015-0502-y.

[22] TKF (Twentse KabelFabriek). *Kunststof Middenspanningskabels*. Jan. 2000. URL: https://www.tkf.nl/files/content/twenpower-nederlands-2015.09.09.115800.pdf.

[23] The Mathworks. *MATLAB*. Version R2020b Update 5 (9.9.0.1592791) win64. Feb. 4, 2021. URL: https://nl.mathworks.com/products/matlab.html.

[24] COMSOL Inc. *COMSOL*. Version 5.3.0.316. Sept. 7, 2017. URL: https://www.comsol.com/.

[25] R. S. Olsen, J. Holboll, and U. S. Gudmundsdóttir. “Dynamic temperature estimation and real time emergency rating of transmission cables”. In: *2012 IEEE Power and Energy Society General Meeting*. 2012, pp. 1–8. DOI: 10.1109/PESGM.2012.6345324.

[26] Soroush Shafiee, Mahmud Fotuhi-Firuzabad, and Mohammad Rastegar. “Investigating the Impacts of Plug-in Hybrid Electric Vehicles on Power Distribution Systems”. In: *IEEE Transactions on Smart Grid* 4.3 (2013), pp. 1351–1360. DOI: 10.1109/TSG.2013.2251483.

[27] Emily Parry and Miles Redfern. “Load management of the electricity supply network using plug-in vehicles”. In: *45th International Universities Power Engineering Conference UPEC2010*. 2010, pp. 1–6.

[28] Elaadnl. 2015. URL: https://elaad.nl/.

[29] MFFBAS (MarktFaciliteringsForum Beheerder Afspraken Stelsel). *Profielen elektriciteit 2022 v1.01*. 2022. URL: https://www.mffbas.nl/custom/uploads/2022/04/Profielen-elektriciteit-2022-v1.01.zip.

[30] KNMI (Koninklijk Nederlands Meteorologisch Instituut). *Meer Zon, Iets Minder Zonkracht*. July 2018. URL: https://www.knmi.nl/over-het-knmi/nieuws/meer-zon-iets-minder-zonkracht.

[31] N.V. Nederlandsche Kabelfabrieken. *Catalogus*. NKF Delft-Holland, 1975.

[32] Stedin. *Internal design policy MV network*.

[33] “IEEE Standard Power Cable Ampacity Tables”. In: *IEEE Std 835-1994* (1994), pp. 1–3151. DOI: 10.1109/IEEESTD.1994.7297793.